Temperature dependence of oxygen isotope fractionation in coccolith calcite: A culture and core top calibration of the genus Calcidiscus

Yaël Candelier, Fabrice Minoletti, Ian Probert, Michaël Hermoso

Temperature Dependence of Oxygen Isotope Fractionation in Coccolith Calcite: A Culture and Core Top Calibration of the genus *Calcidiscus*

Yaël Candelier[1, 2, *], Fabrice Minoletti[1, 2], Ian Probert[3], Michaël Hermoso[4]

[1] UPMC Univ Paris 06 – UMR 7193 ISTeP, 4 Place Jussieu, Case postale 116, 75005 Paris, France.

[2] CNRS – UMR 7193 ISTeP, 4 Place Jussieu, Case postale 116, 75005 Paris, France.

[3] UPMC Univ Paris 06 and CNRS – FR 2424 Station Biologique de Roscoff, Place Georges Teissier, 29682 Roscoff, France.

[4] University of Oxford - Department of Earth Sciences, South Parks Road, OX1 3AN Oxford, United Kingdom.

[*] Corresponding author. Email: yael.candelier@upmc.fr. Phone: +33 (0) 1 44 27 27 60.

ABSTRACT

Reconstructions of seawater temperature based on measurement of oxygen isotopes in carbonates mostly derive from analyses of bulk sediment samples or manually picked foraminifera. The temperature dependence of ^{18}O fractionation in biogenic calcite was first established in the 1950s and the objective of the present study is to re-evaluate this temperature dependence in coccolith calcite with a view to developing a robust proxy for reconstructing "vital effect"-free $\delta^{18}O$ values. Coccoliths, the micron-sized calcite scales produced by haptophyte algae that inhabit surface mixed-layer waters, are a dominant component of pelagic sediments. Despite their small size, recent methodological developments allow species-specific separation (and thus isotopic analysis) of coccoliths from bulk sediments. This is especially the case for *Calcidiscus* spp. coccoliths that are relatively easy to separate out from other sedimentary carbonate grains including other coccolith taxa. Three strains of coccolithophores belonging to the genus *Calcidiscus* and characterised by distinct cell and coccolith diameters were grown in the laboratory under controlled temperature conditions over a range from 15 to 26 °C. The linear relationship that relates ^{18}O fractionation to the temperature of calcification is here calibrated by the equation: $T\ [°C] = -5.83 \times (\delta^{18}O_{Calcidiscus} - \delta^{18}O_{medium}) + 4.83$ ($r = 0.98$). The slope of the regression is offset of ~ –1.1 ‰ from that of equilibrium calcite. This offset corresponds to the physiologically induced isotopic effect or "vital effect". The direction of fractionation towards light isotopic values is coherent with previous reports, but the intensity of fractionation in our dilute batch cultures was significantly closer to equilibrium compared to previously reported offset values. No significant isotopic difference was found between the three *Calcidiscus* coccolithophores, ruling out a control of the cell geometry on oxygen isotope fractionation within species of this genus. This also indicates that our culture calibration may be applied to all *Calcidiscus* coccoliths found in the sediment. We compared the culture calibration to $\delta^{18}O$ measured from near-monogeneric *Calcidiscus* fractions separated out from core top sediments. We found concordant ^{18}O fractionation factors for the core top calibration with a good linear coefficient ($r = 0.94$). The near-monogeneric *Calcidiscus* assemblages seem, however, to record slightly heaviest $\delta^{18}O$ values compared to the data of culture

study. This discrepancy may be due to a possible seasonality effect on the production of *Calcidiscus* coccoliths. The uncertainty of the calibration is of similar magnitude to those of other proxies used for SST reconstruction, such as foraminiferal $\delta^{18}O$ or the alkenone undersaturation index. This confirms that coccoliths can be used as a complementary or alternative substrate to foraminiferal shells for isotopic analyses. Comparing $\delta^{18}O$ of coccoliths to these other SST proxies, or developing an interspecific comparison of coccolith geochemistry may give insights into the carbonate chemistry of seawater through key periods of the geological record.

1. INTRODUCTION

Subsequent to the pioneer work by Urey (1947), Emiliani (1955, 1966) attempted the first palaeoceanographic application of oxygen isotopes ($\delta^{18}O$) in carbonates to reconstruct sea surface temperatures (SSTs). Laboratory experiments have empirically established equations linking temperature of calcification to fractionation of oxygen isotopes in carbonates (Erez and Luz, 1983; Bemis et al., 1998; Ziveri et al., 2003; Coplen, 2007; Day and Henderson, 2011). In the natural environment, however, the $\delta^{18}O$ of carbonates cannot be regarded as a direct proxy for SSTs because variations in the ice volume, the regional hydrographic regime and consecutive changes in the inventory of $^{18}O/^{16}O$ in seawater exert a primary control on $\delta^{18}O$ in carbonates. As a consequence of the ambiguity of the proxy, down-core reconstruction of SSTs still requires knowledge of past $\delta^{18}O$ of seawater. Nevertheless, attempts to interpret $\delta^{18}O$ of carbonate represent a large body of literature in palaeoclimatologic reconstructions (Imbrie et al., 1984; Zachos et al., 2001; Wang et al., 2008; Dera et al., 2011). Notably, this geochemical tool has provided an insightful dataset documenting ocean palaeotemperatures, as the long-term stacked oxygen isotope from benthic foraminiferal record used as reference for the Cenozoic climate (Zachos et al., 2001; Zachos et al., 2008).

Most of $\delta^{18}O$ data generated from pelagic carbonates have been measured from bulk carbonate or monospecific signals by measurements on hand-picked foraminifera. In addition to shells of foraminifera, coccoliths, the micron-sized calcite scales produced by the coccolithophores, are

abundant microfossils in all pelagic sediments since the Jurassic. The main reason that stable isotopes in coccoliths have been underexploited is the challenge of separating out micron-sized particles from bulk sediments. In recent years, however, methodological advances have made it possible to obtain near-monospecific assemblages of coccoliths from mixed sediment samples (Minoletti et al., 2001; Stoll and Ziveri, 2002; Halloran et al., 2009; Minoletti et al., 2009) opening the possibility of exploiting the potential of fossil coccoliths for reconstruction of palaeoclimate.

Coccolithophores are photosynthetic algae and most species calcify within the mixed-layer. Therefore, they have the potential to capture physico-chemical conditions, including temperatures prevailing in the uppermost water column. Coccoliths are composed of highly imbricated monocrystalline calcite elements without internal porosity, making them more resistant to dissolution and overgrowth than foraminiferal shells (McIntyre and McIntyre, 1970; Schneidermann, 1977; Broecker and Clark, 2009). Primary isotopic signals are, hence, better preserved in coccoliths than in foraminiferal shells, the latter being prone to diagenetic overprinting by overgrowth and porosity filling (Bouvier-Soumagnac and Duplessy, 1985; Caron et al., 1990; Wefer and Berger, 1991). Foraminifera species used to retrieve surface water conditions are typically prone to dissolution (Kucera, 2007), while resistant species tend to migrate and record temperatures from deeper waters (Henderson, 2002; Barker et al., 2005; Farmer et al., 2007). The widespread distribution of coccoliths in sediments, including at high latitudes where foraminifera are usually rare, and their abundance in high deposition rate sedimentary regimes, where foraminifera are diluted by detrital material, also make coccoliths attractive for use in palaeoenvironmental research.

Offsets from equilibrium conditions have been recorded in the oxygen isotope signatures of most biomineralisations, especially in coccolithophorid and foraminiferal calcite (Dudley and Goodney, 1979; Dudley et al., 1986; Bemis et al., 1998; Elderfield and Ganssen, 2000; Ziveri et al., 2003). The amplitude of the biologically induced ^{18}O fractionation or vital effect (Epstein et al., 1951, 1953; Urey et al., 1951), as well as the inter- and intraspecific variability of $\delta^{18}O$ may be high. In coccolith calcite, these biologically induced disequilibria are explained by kinetic fractionation occurring during the uptake of carbonate species into the cell and subsequently into the coccolith vesicle (Rickaby et al., 2010). In foraminiferal calcite, disequilibria may originate from the activity of photosynthetic

104 symbionts, from addition of gametogenic calcite, from reutilisation of respired CO_2 for calcification or
105 from a salinity effect (Erez, 1978; Duplessy et al., 1981; Spero and Lea, 1993; Wolf-Gladrow et al.,
106 1999; Arbuszewski et al., 2010).
107 In the present study, we attempt the first combined culture and field calibration of the temperature
108 dependence of ^{18}O fractionation for the coccolithophore genus *Calcidiscus* Kamptner. This
109 cosmopolitan genus produces relatively large coccoliths with diameters between 3 and 11 µm (Geisen
110 et al., 2004) that are relatively easily separated from other sedimentary components (including from
111 coccoliths of other taxa) using the recently developed microseparation protocol of Minoletti et al.
112 (2009). Its widespread geographic distribution and low susceptibility to dissolution make *Calcidiscus*
113 a good candidate for attempting temperature estimates during time periods of stable oceanic $\delta^{18}O$, i.e.
114 without significant changes in the waxing and waning of the ice sheets. The genus contains two
115 formally described extant species, *C. quadriperforatus* (Kamptner) Quinn & Geisen and *C. leptoporus*
116 (Murray & Blackman) Loeblich & Tappan, the former having large coccoliths (7-11 µm diameter)
117 with a zone of obscured sutures around the central area, and the latter having smaller coccoliths (5-8
118 µm) with continuous sutures. These species were classified as intra-specific variants (morphotypes or
119 sub-species sensu Knappertsbusch et al., 1997) of *C. leptoporus* until Sáez et al. (2003) demonstrated
120 significant genetic variation between them, warranting species level separation. A third species likely
121 exists within the genus, characterised by small coccoliths (3-5 µm) with kinked sutures, but in the
122 absence of genetic data it has not yet been formally described and is commonly referred to as
123 "*Calcidiscus* sp. small".
124 To date, very few studies have measured the intensity of isotopic fractionation in *Calcidiscus* coccolith
125 calcite. Two studies have reported interspecific variability in $\delta^{18}O$ of coccolith calcite from
126 experiments using laboratory culture strains (Dudley et al., 1986; Ziveri et al., 2003). From previous
127 culture experiments using *C. leptoporus* (sensu lato), coccolith calcite has consistently been shown to
128 record lighter oxygen isotopes relative to equilibrium calcite, but contradictory results have been
129 reported about the amplitude of this offset (Dudley et al., 1986; Ziveri et al., 2003). We cultured and
130 analysed three strains of *Calcidiscus* (two strains of *C. leptoporus* and one of *C. quadriperforatus*) that
131 differ in both coccosphere and coccolith sizes. As both cell size and genetic diversity may control the

intensity of ^{18}O fractionation (Rickaby et al., 2010), this interspecific comparison would allow determination of whether our calibration of ^{18}O fractionation is transferable to sediment fractions containing different *Calcidiscus* coccoliths.

2. MATERIALS AND METHODS

Three environmental and sedimentary variables need to be constrained in order to investigate temperature dependence on ^{18}O fractionation: temperature of calcification, $\delta^{18}O$ of seawater ($\delta^{18}O_{sw}$) and $\delta^{18}O$ of carbonate ($\delta^{18}O_{carb}$). The temperature dependence of ^{18}O fractionation is expressed as the offset between $\delta^{18}O$ of coccolith calcite and $\delta^{18}O$ of seawater at distinct temperatures. In culture, each of these parameters can be directly measured, whereas for core top sediments only the $\delta^{18}O$ of coccoliths can be directly evaluated. This implies that data on temperature and $\delta^{18}O$ of the surface water mass in which the calcite was formed is retrieved from oceanographic databases.

2.1. Laboratory Culture Study

Dilute batch cultures of three clonal, heterococcolith-producing strains of *Calcidiscus* from the Roscoff Culture Collection (http://www.sb-roscoff.fr/Phyto/RCC/) were conducted. The two strains of *C. leptoporus* originated from the Japanese Pacific coast (RCC 1162) and from the Atlantic Ocean, offshore South Africa (RCC 1129), and the *C. quadriperforatus* strain was isolated from the Mediterranean Sea (RCC 1157). Experiments were conducted at six temperatures for RCC 1162 (15, 17, 20, 23, 25 and 26 °C) at the *Station Biologique de Roscoff*, and three temperatures for RCC 1129 and RCC 1157 (15, 20 and 25 °C) at Oxford University Department of Earth Sciences. For each strain, two replicate cultures were grown at each temperature. No growth was obtained for RCC 1157 at 25 °C. For RCC 1162, batch cultures carried out in 2.7 L Nalgene® polycarbonate flasks, without headspace. For the other two strains, 600 mL polycarbonate vessels were used, again without headspace. The culture medium was identical for all experiments, using enriched English Channel

seawater. Trace metal and chelator enrichments corresponded to K/6 (Keller et al., 1987) with omission of Tris and Si (Probert and Houdan, 2004). Nitrate and phosphate concentrations were adjusted to respectively 100 µmol.L^{-1} and 6.25 µmol.L^{-1}. The level of vitamins was that of f/2 (Guillard, 1975). Before sterilisation, achieved by tyndallisation and filtering through a single-use 0.22 µm pore-size sterilisation device, media were bubbled with atmospheric air for 24 hours and the *p*H was corrected to 8.2 (total scale) by addition of 0.2 M NaOH. Cultures were illuminated by daylight fluorescent bulbs at a light intensity of ~ 150 µmol photons.m^{-2}.s^{-1} (corresponding to the photic zone irradiance value) with a 14/10 light/dark cycle.

The cultures were slowly acclimated (0.5 °C per day) and maintained at the target temperature in their exponential phase of growth for at least 10 generations before initiation of the experiments. The initial cell density at inoculation was ~ 50 cells per mL. Aliquots of the culture medium were sampled at the beginning and the end of the experiments, filtered through a 0.22 µm syringe filter and kept at 4 °C until $\delta^{18}O_{sw}$ and *p*H measurements. During the experiment, the cell density of RCC 1162 was measured daily by optical counting under an inverted microscope (magnification x 40) using a Sedgwick Rafter slide. For the other two strains, cell concentrations were measured using a Beckman Coulter Counter II. Cultures were harvested when cell density reached ~ 6,000 cells.mL^{-1}. At this stage, the algal population was still at the early stage of the exponential growth phase, and under nutrient- and dissolved inorganic carbon-replete conditions.

2.2. Core Top Sediment Study

2.2.1. Sediment Samples and Depositional Environments

We used sediments from ten distinct locations (Fig. 1), eight from the North Atlantic Ocean (Holes SU90-03; SU90-08; V04-08; V30-76; V30-97; MD95-2038; SU81-28; NO75-14), and two from the western Indian Ocean (Holes MD104-AT960028, MD104-AT960029). Details for each site and reference to age models are given in Table 1 and in electronic annex (electronic annex Table A.1). Core locations were chosen from manifold surface water mass settings on the basis of temperature and

187 $\delta^{18}O_{sw}$ values.

188 The Atlantic sites are located in the subtropical North Atlantic Gyre under temperate climatic
189 conditions (Fig. 1). The two Indian Ocean samples were recovered on the continental slope of the
190 northern Somali Basin. Present-day oceanographic conditions in this area are warm and nutrient-rich
191 surface water masses and the presence of a reverse monsoon system driving coastal upwelling (Fischer
192 et al., 1996; Schott et al., 2001; Peeters et al., 2002). The saturation state of bottom waters with respect
193 to carbonate ion ($\Delta [CO_3^{2-}]$) averaged from the GLODAP bottle dataset (Key et al., 2004; Sabine et al.,
194 2005) was calculated following the recommendations of Archer (1996) and Mekik et al. (2010).
195 Selecting sediments laid down in high $\Delta [CO_3^{2-}]$ waters is a prerequisite for ensuring that calcareous
196 particles had undergone minimal dissolution during export to the seafloor. It is important to take this
197 precaution to avoid fragmentation of foraminiferal shells because their debris may pervade into the
198 size range of coccoliths, typically between 5 and 20 microns (Minoletti et al., 2009). For most of the
199 sites, bottom waters are highly saturated with respect to carbonate ion ($\Delta [CO_3^{2-}] > 25$ μmol.kg-1),
200 except for site NO75-14 and for the two Indian Ocean sites (Table 1).

201

202 *2.2.2. Assessing $\delta^{18}O$ and Temperature of the Surface Water Column*

203

204 All of the sediments used in this study were sampled from the first few centimetres of the cores. The
205 ages of the Atlantic sites have been attributed to Late Holocene to recent (<5 kyr) by radiocarbon
206 dating, oxygen stratigraphy and deposition rates measured or estimated from surrounding cores
207 (CLIMAP Project Members, 1976; Imbrie et al., 1989; Broecker et al., 1991; Gruetzner et al., 2002;
208 Mathien-Blard and Bassinot, 2009; see Table 1). For the Indian Ocean box cores, high sedimentation
209 rate in the area (20-25 cm/kyr) and radiometric dates measured on surrounding cores indicate an age
210 younger than 0.5 kyr (Vénec-Peyré et al., 1995; Klöcker et al., 2006). Due to these recent ages,
211 carbonates were assumed to have been formed in water masses characterised by physico-chemical
212 properties close to present day conditions.
213 For each core location, we retrieved mean annual values and seasonal variability of temperature and
214 $\delta^{18}O_{sw}$ from 0-50 m where most of the *Calcidiscus* population lives and calcifies (Knappertsbusch and

Brummer, 1995; Haidar et al., 2000; Haidar and Thierstein, 2001). Seawater temperatures were retrieved from the World Ocean Atlas 2009 (Locarnini et al., 2010). Mean seawater oxygen isotope ratios ($\delta^{18}O_{sw}$) were retrieved from the global 1° x 1° gridded compilation of LeGrande and Schmidt (2006).

2.2.3. Obtaining Near-Monogeneric Fractions of Calcidiscus from Core Top Sediments

We applied the protocol described in Minoletti et al. (2001; 2009) based on cascade microfiltering steps to concentrate *Calcidiscus* coccoliths from the sediments. About 5 g of bulk material were suspended in deionised water adjusted to *p*H 8 by addition of ammonia, and gently stirred until complete disaggregation of the sediment. This suspension was sieved through 315 and 160 µm nylon mesh, and then pre-filtered through 20 and 10 µm Millipore® polycarbonate membranes. The coarse fractions retained almost all foraminifera (entire tests and fragments). The fine fraction (<10 µm) was then successively filtered through 8, 5 and 3 µm polycarbonate membranes to concentrate *Calcidiscus* in the fractions 3-5 µm and 5-8 µm. After separation, smear-slides from each fraction were made using the technique described by Koch and Young (2007). Relative abundance and the enrichment in *Calcidiscus* were estimated by counting > 500 particles under cross-polarised light using a Zeiss Axioscope 40® equipped with a 63 × Plan-Neofluar objective. The preservational state of coccoliths (etching and overgrowth) and potential presence of diagenetic crystals in the separated fractions were checked using a Zeiss Supra® 55VP Scanning Electron Microscope (SEM).

2.3. Isotopic measurements

Stable isotopes from about 250 µg of culture residue or near-monogeneric sediment fractions were analysed on a VG Isogas Prism II mass spectrometer with an on-line VG Isocarb at Oxford University. Samples were first cleaned using 10 % hydrogen peroxide (H_2O_2) and dried at 60 °C for at least 30 minutes. In the instrument they were reacted with purified phosphoric acid (H_3PO_4) at 90 °C. Calibration to V-PDB standard via NBS-19 was undertaken daily using the Oxford in-house (NOCZ)

243 Carrara marble standard. The oxygen isotope composition of water samples was measured from the
244 CO_2 in the headspace equilibrated with a 0.5 mL aliquot in Exetainer® tubes using Gas Bench II
245 coupled to a Delta V Advantage mass spectrometer at Oxford University. The results ($\delta^{18}O_{sw}$) are
246 expressed against V-SMOW. Two international water standards (IA-RO53 and IA-RO54; $\delta^{18}O$ = –
247 10.18 ‰ and +0.56 ‰ [V-SMOW], respectively) were run to perform a two-point external calibration
248 for the raw isotopic results. Reproducibility of replicated standards was usually better than 0.1 ‰ for
249 $\delta^{18}O_{carb}$ and 0.2 ‰ for $\delta^{18}O_{sw}$. The fractionation between calcite and water is reported as $\delta^{18}O_{carb}$ [V-
250 PDB] – $\delta^{18}O_{sw}$ [V-SMOW], referred to as "^{18}O fractionation" hereafter. Hence, the analytical error
251 associated to the term $\delta^{18}O_{carb} - \delta^{18}O_{sw}$ is the square root of the term $(0.1^2 + 0.2^2)$, and is about 0.22 ‰.
252
253 ## 2.4. Expression of ^{18}O fractionation factors
254
255 Reporting the isotopic fractionation against equilibrium calcite ("offset from equilibrium" hereafter) is
256 common procedure in palaeoceanographic and biogeochemical studies. The amplitude of this offset
257 from equilibrium is commonly assigned to the biologically induced fractionation or vital effect (Bemis
258 et al., 1998; Stoll and Ziveri, 2004). However, a wide range of equilibrium equations is available in
259 the literature and the definition of equilibrium conditions is highly subjective (see Zeebe and Wolf-
260 Gladrow, 2001 for a synthesis and subsequent work by Dietzel, 2009 and Day and Henderson, 2011;
261 electronic annex Fig. A.1). Nowadays, the most commonly used equation is that of Kim and O'Neil
262 (1997). In this study, we applied the conversion from the "$10^3 \times \ln \alpha$" notation to "$\delta - \delta$" as done by
263 Bemis et al. (1998).
264
265 (1) $\delta^{18}O_{equilibrium}$ [V-PDB] – $\delta^{18}O_{sw}$ [V-PDB] = $(0.0009 \times T^2) - (0.2468 \times T) + 3.7434$
266
267 where T is the temperature of calcification (in °C) and $\delta^{18}O_{sw}$ the oxygen isotope composition of
268 seawater on the V-PDB scale. Conversion from the V-SMOW to the V-PDB scale is obtained by
269 subtracting 0.27 ‰ (Hut, 1987). Zeebe (1999) demonstrated that ^{18}O fractionation in minerals is

dependent on the medium *p*H. This relationship means that calcite precipitated from higher *p*H conditions exhibits less ^{18}O fractionation in comparison with calcite precipitated at lower *p*H. This theoretical mechanism has also proven to be true for foraminiferal calcite with a decrease of -1.1 ‰ in $\delta^{18}O_{carb}$ as a result of a rise of one *p*H unit (Spero et al., 1997). Since our culture experiments were conducted at *p*H 8.2, we adjusted the equilibrium equation originally determined for *p*H 7.8 in Kim and O'Neil (1997) by subtracting 0.4 ‰ from the intercept of (Eq. 1) to account for this *p*H effect and to allow comparison between this equilibrium reference and our culture data. In the following account, we report the intensity of the vital effect as the offset of $\delta^{18}O$ in coccoliths from this latter equilibrium line. Equation 1 including the –0.4 ‰ *p*H correction gives:

(2) $\delta^{18}O_{equilibrium}$ [V-PDB] – $\delta^{18}O_{sw}$ [V-PDB] = $(0.0009 \times T^2) - (0.2468 \times T) + 3.3434$

with temperature in °C.

3. RESULTS

3.1. Calibrating the $\delta^{18}O$ – Temperature Relationship in Cultured *Calcidiscus*

3.1.1. Coccolithophore Growth and Evolution of the Culture Medium

Three strains of *Calcidiscus* with distinct cell and coccolith sizes were grown in the laboratory over a range of temperatures from 15 to 26 °C. For the three strains, the temperature had an influence on growth rate (μ), which ranged from 0.1 day^{-1} at the lowest temperature to 0.45 day^{-1} at the highest temperature (see electronic annex Table A.2 for details) that is a classical physiological response of most of coccolithophores species (Buitenhuis et al., 2008). The smallest strain (RCC 1129 with a mean coccosphere diameter 15 μm; coccolith diameter 5.8 μm) was the faster growing compared to the larger strains (RCC 1162 and RCC 1157; both mean coccosphere diameter 20-21 μm and coccolith diameter 8.8 μm). The experiments were harvested at a cell density of about 6,000 $cells.mL^{-1}$ and the

297 mass of residues was about 10 to 25 mg including coccoliths as particulate inorganic carbon (PIC) and
298 organic matter as particulate organic carbon (POC). Due to the very low cell density in our batch
299 cultures, which is a prerequisite for minimising effects of varying carbonate chemistry in laboratory
300 cultures of coccolithophores (Langer et al., 2006; Barry et al., 2010), we did not obtain enough
301 residues to perform measurements of the PIC/POC ratio. In any case, the partitioning of carbonate ion
302 species between calcite and organic matter has been proven to impact carbon isotope fractionation, but
303 not that of oxygen isotopes (Rickaby et al., 2010). Furthermore, it can be assumed that the PIC/POC of
304 our culture residues was comparable between batches because the primary factor governing this ratio
305 is irradiance (Langer et al., 2006), and all of our experiments were conducted under similar light
306 intensity and identical photoperiod.
307 The typical drift in oxygen isotope composition of the medium during the experiments was less than
308 0.1 ‰ (see electronic annex Table A.2). This is within the analytical error of $\delta^{18}O$ measurements, and
309 is not significant. In a closed culture vessel (i.e., with no headspace to avoid dissolved inorganic
310 carbon (DIC) re-equilibration with the atmosphere), the *p*H reflects the relative proportion of
311 dissolved carbon dioxide, bicarbonate and carbonate ions in the medium. Constant *p*H through the
312 experiments thus provides evidence of the stability of the carbonate system and very low amount of
313 DIC scavenged by *Calcidiscus* during growth (photosynthesis and calcification).
314
315 ### *3.1.2. Temperature Control on ^{18}O Fractionation of Cultured Calcidiscus*
316
317 The $\delta^{18}O$ of *Calcidiscus* coccolith calcite showed an unequivocally linear relationship with
318 temperature. The colder the temperature at which calcification took place, the heavier the $\delta^{18}O$ of
319 coccoliths, a classical result also observed for equilibrium calcite (Fig. 2). It is important to point out
320 that no significant (greater than analytical error) offsets were observed when comparing the three
321 strains: the oxygen-isotope fractionation in coccoliths of *C. quadriperforatus* (RCC 1157) was
322 indistinguishable from that in coccoliths of *C. leptoporus* (RCC 1129 and RCC 1162) (Fig. 2).
323 Quantitatively, the amplitude of ^{18}O fractionation ($\delta^{18}O_{Calcidiscus} - \delta^{18}O_{sw}$) ranged from –1.57 ‰ at

15 °C to –3.71 ‰ at 25 °C (EA-2). These offsets from seawater $\delta^{18}O$ were dictated by temperature in a linear-fashion as illustrated by a remarkably high regression coefficient (r) of 0.98 (Fig. 2). This correlation and the low variability between replicates indicate that the temperature dependence of ^{18}O fractionation in *Calcidiscus* calcite in culture experiments is reproducibly predictable using the following equations:

(3) $\delta^{18}O_{carb}$ [V-PDB] – $\delta^{18}O_{medium}$ [V-SMOW] = $-0.17 \times T + 0.83$ ($r = 0.98$; *p*-value < 2×10^{-15})
with temperature in °C.

(4) $\varepsilon^{18}O_{carb–medium} = -0.18 \times T + 31.76$
with temperature in °C.

The Root Mean Square Error (RMSE) of the distribution (n = 22) indicates a residual of about 0.8 °C indicating the good accuracy of the culture calibration. The slope of this calibration line means that an increase of 1 °C in temperature results in a decrease of 0.17 ‰ in $\delta^{18}O_{carb}$. Comparison of the slopes from our culture data and equilibrium at *p*H 8.2 reveals a relatively constant offset, irrespective of temperature, of –1.1 ‰ (Fig. 2).

3.2. Quantifying the Isotopic Disequilibrium of *Calcidiscus* from Core Top Sediments

3.2.1. Retrieving Surface Mixed-Layer Temperature and $\delta^{18}O_{sw}$

Averaged annual temperatures and $\delta^{18}O$ of seawater of the 0-50 m depth range contrasted between the Atlantic and Indian Ocean sites (Fig. 3a; Fig. 3b), ranging from 15.9 °C to 26.5 °C for temperature, and 0.49 ‰ to 1.08 ‰ for $\delta^{18}O_{sw}$ (WOA database; LeGrande and Schmidt, 2006; Locarnini et al., 2010). Details for each site are given in Table 2.

3.2.2. Composition of the Microseparated Fractions and Preservational State of Coccoliths

The original sediments contained coccoliths from a variety of different coccolithophore species (Fig. 4a; Fig. 4b). By applying the microseparation technique, we successfully obtained subsamples enriched in *Calcidiscus* in the 5-8 µm and 3-5 µm fractions (Fig. 4c and Fig. 4d). In some of the 3-5 µm fractions, however, the purity of *Calcidiscus* was not great enough to regard them as near-monogeneric, and as a consequence these were discarded from our calibration (see electronic annex Table A.3).

The best enrichment in *Calcidiscus* is generally achieved in the 3-8 µm size spectrum due to the fact that there are no dominant or even abundant coccoliths from other taxa that share this size spectrum, with the notable exception of *Helicosphaeara* spp. Noelhaerhadaceae coccoliths (*Gephyrocapsa* sp. and *Emiliania huxleyi*) are usually gathered in microseparated fractions smaller than 3 µm. *Coccolithus pelagicus* and most foraminiferal fragments are retained in the coarser fractions (8-10 µm and 10-20 µm, respectively).

Coccoliths contained in our 3-5 µm and 5-8 µm fractions cannot straightforwardly be assigned to *Calcidiscus* sp. small and *C. leptoporus*, respectively, due mainly to disarticulation of the two shields and/or fragmentation of coccoliths that occurs naturally in the sediment or during the microseparation protocol. As a result, the 5-8 µm fraction tends to be dominated by entire specimens of *C. leptoporus* and some *C. quadriperforatus* shields, while the 3-5 µm fraction tends to be a mixture of *Calcidiscus* sp. small (<5 µm) and isolated shields of *C. leptoporus*.

For the Atlantic Ocean samples (Table 3), the relative abundance of *Calcidiscus* spp. ranged from 50 % to 86 % (mean 72 %). The secondary components were coccoliths of *Helicosphaera* spp., *Pontosphaera* spp. and *Coccolithus pelagicus* in the 5-8 µm fractions, and small *Gephyrocapsa* spp. and a few *Emiliania huxleyi* coccoliths in the 3-5 µm fractions. For the Indian Ocean samples, the relative abundance of *Calcidiscus* spp. ranged from 47 % to 80 % (mean 61 %). These lower values result from higher abundance of small foraminiferal fragments in bulk samples likely due to slightly more corrosive bottom waters in this area. Secondary calcareous components in the 5-8 µm and 3-5 µm fractions mainly consisted of small foraminiferal fragments and tiny Noelaerhabdaceae coccoliths,

379 respectively (Table 3).

380 In all fractions presented in Fig. 5, the abundances in *Calcidiscus* spp. were very high compared to the
381 low initial abundance (~ 5 %) of this taxon in bulk samples (Fig. 4a), corresponding to a mean 13-fold
382 enrichment in this taxon.

383 A key parameter to consider when dealing with the purity of the isotopic signal is the contribution of
384 *Calcidiscus* spp. to the carbonate in the separated fractions. The individual mass of *Calcidiscus*
385 coccoliths is greater than that of all other coccoliths of secondary importance observed in our
386 microseparated fractions with the exception of *Coccolithus pelagicus* (Young and Ziveri, 2000) and
387 greater than that of foraminiferal fragments. For example, the mass of *C. leptoporus* coccoliths is
388 about 8-fold greater than that of coccoliths of the family Noelaerhabdaceae such as *Gephyrocapsa*
389 *oceanica* that coexisted in the 3-5 μm fractions (Young and Ziveri, 2000). The extent to which $\delta^{18}O$
390 measurements can be attributed to *Calcidiscus* spp. in microseparated fractions was therefore greater
391 than would be inferred from the relative abundance of this taxon. In SEM images, we observed slight
392 etching and isolated shields, a common preservational feature for this genus (McIntyre and McIntyre,
393 1970). These features were likely induced by the separation protocol because preservation was better
394 in untreated bulk samples, but do not affect the measured isotopic signatures (Minoletti et al., 2009).
395 Importantly, no overgrowth was seen on coccoliths, and no diagenetic components observed in
396 separated fractions (Fig. 4c; Fig. 4d). The $\delta^{18}O$ of *Calcidiscus* spp. can hence be regarded as pristine.
397 The dominance of *Calcidiscus* spp. in the separated fractions (defined by both high relative abundance
398 and large relative size, and hence mass) and their good state of preservation mean that the oxygen
399 isotopic signatures measured on *Calcidiscus*-dominated fractions can be taken to reflect the original
400 composition (temperature and $\delta^{18}O_{sw}$) of the surface waters in which they calcified.

401

402 ### *3.2.3. Oxygen Isotope Composition and ^{18}O Fractionation in Sediments*

403

404 Large oxygen isotope offsets were observed between microseparated fractions of the sediments. The
405 range of $\delta^{18}O_{carb}$ over all size fractions was as high as 3 ‰ (e.g. site SU81-28, Table A.3). Taken at

face value, this would indicate that biogenic carbonate particles comprised in a sediment may record substantially different temperatures, up to 12 °C. The $\delta^{18}O$ of the bulk assemblage is, for most samples, close to that of the finest (less than 2 or 3 μm) fraction owing to the dominance of this size class in pelagic sediments (see discussion by Minoletti et al., 2009). These finest fractions are dominated by small coccoliths such as those of *Emiliania huxleyi* and *Gephyrocapsa oceanica*. However, the isotopic composition of this size fraction has proven to be difficult to interpret for old and potentially diagenetically altered sediments due to the relatively high abundance of the so-called "micarbs" that derive from coccolith fragmentation or correspond to diagenetic precipitations (Minoletti et al., 2004; Minoletti et al., 2005; Beltran et al., 2009; Hermoso et al., 2009). In contrast, the size fractions bracketing 5 μm usually offer the opportunity to generate isotopic measurements free of micarbs and foraminiferal fragments. In the present study, *Calcidiscus* assemblages were characterised by a mean $\delta^{18}O$ offset of –1.46 ‰ (ranging from –2.25 ‰ to –0.82 ‰) with respect to bulk sediments. For the Atlantic Ocean sites (averaged annual temperature of about 18.4 °C), measured $\delta^{18}O$ of *Calcidiscus* fractions ranged from –1.83 ‰ to –0.59 ‰ (Fig. 5). In the Indian Ocean sites (averaged annual temperature of about 26.1 °C), the $\delta^{18}O$ values of *Calcidiscus* fractions ranged from –2.94 ‰ to –2.53 ‰. There was no systematic isotopic difference between the 3-5 μm and 5-8 μm fractions (Fig. 5; Fig. 6). Considering the different abundances of *Calcidiscus* species within these fractions, it does not appear that a species-specific effect exists within the *Calcidiscus* genus, a conclusion that is consistent with that from our culture study.

The ^{18}O fractionation between *Calcidiscus* coccolith calcite and seawater, expressed as the $\delta^{18}O_{carb} - \delta^{18}O_{sw}$, ranged from –2.90 ‰ to –1.42 ‰ with a mean offset of –1.89 ‰ for the Atlantic sites, and –3.48 ‰ to –3.07 ‰ with a mean offset of –3.21 ‰ for the Indian Ocean sites. The 24 points of our core top calibration gave an overall good linear relationship between temperature of calcification and ^{18}O fractionation (Eq. 5; Fig. 6). The coefficient of the linear regression (r = 0.94) is remarkably high for an environmental study.

(5) $\delta^{18}O_{carb}$ [V-PDB] – $\delta^{18}O_{sw}$ [V-SMOW] = $-0.16 \times T + 0.97$ (r = 0.94; *p*-value < 2×10^{-11})

with temperature of the 0-50 m water mass in °C. The RMSE of the distribution (n = 24) indicates a residual of about 1.4 °C.

4. DISCUSSION

4.1. Comparison with Previously Reported Fractionation Factors for *Calcidiscus*

To date, only two studies have documented the effect of temperature on ^{18}O fractionation in coccoliths of *Calcidiscus* in culture experiments (Dudley et al., 1986; Ziveri et al., 2003; Fig. 2). The latter study included several different coccolithophore species, but *Calcidiscus* was only cultured at 17 °C. Note that the strain used by Ziveri et al. (2003) (PC11M3 = RCC 1153) was designated at the time as *C. leptoporus*, but has subsequently been reclassified as *C. quadriperforatus*. Dudley et al. (1986) reported a linear correlation between temperature and ^{18}O fractionation for *C. leptoporus* cultured over a range from 17 to 28 °C with 4 intermediate temperatures and established the following equation:

(6) $\delta^{18}O_{carb}$ [V-PDB] – $\delta^{18}O_{sw}$ [V-SMOW] = –0.14 × T – 1.02 (r = 0.75; RMSE = 2.4 °C)

In all culture studies to date, *Calcidiscus* $\delta^{18}O$ values are lower (i.e. more negative) than equilibrium calcite (Fig. 2). Dudley et al. (1979) assigned *C. leptoporus* to a "light group" along with other species producing large cells such as *Coccolithus pelagicus*. In contrast, the "heavy group" ($\delta^{18}O$ more positive than equilibrium) comprised species that produce small cells such as *Emiliania huxleyi* and *Gephyrocapsa oceanica* (Dudley et al., 1986; Ziveri et al., 2003; Stoll and Ziveri, 2004; electronic annex Fig. A.1). The single data point produced by Ziveri et al. (2003) for *C. quadriperforatus* gave an isotopic offset from equilibrium (Eq. 2) of –0.7 ‰, which is of the same order of disequilibrium as our results (–1.1 ‰). In contrast, Dudley et al. (1986) obtained a mean fractionation of –2.2 ‰ with respect to equilibrium (Fig. 2). This discrepancy in the vital effect of ~ 1 ‰ is much greater than analytical error, and would correspond to a difference of about 4 °C when translated into a temperature

460 estimate.

461 Dudley et al. (1986) produced a considerable amount of culture data on *C. leptoporus*, but the
462 dispersion between replicates was relatively high (Fig. 2), with offsets up to 1.5 ‰. At face value, this
463 would imply that the control of the temperature during the experiments was ± 3 °C, which appears to
464 be highly unlikely. Given the lack of information on the strain used by Dudley et al. (1986), it is not
465 possible to determine to which *Calcidiscus* species it actually belonged. However, the present study
466 shows that the different *Calcidiscus* species of contrasting origins and morphologies give consistent
467 results and indicates that the use of different strains in different studies is very unlikely to be the
468 reason for the significant isotopic differences recorded.

469 Unfortunately, little is mentioned in Dudley et al. (1986) about the nature of the culturing set-up and
470 evolution of the culture medium. The only relevant information is that the authors grew *C. leptoporus*
471 in relatively high macronutrient concentrations (P = 36 µmol.L^{-1}. and N = 880 µmol.L^{-1})
472 corresponding to f/2 medium composition (Guillard, 1975). Macronutrients, notably phosphate, are
473 known to influence calcification (Kayano and Shiraiwa, 2009). This methodological point may
474 suggest a possible link between inhibition of the calcification and intensity of kinetic ^{18}O partitioning
475 under high phosphate levels. In contrast, our experiments and those of Ziveri et al. (2003) were
476 conducted in much more diluted (about eight-fold lower) macronutrient concentrations, closer to
477 natural conditions and gave similar results. A recent work by Langer et al. (2012) has demonstrated
478 limited effect on the calcification of *C. leptoporus* under phosphate limitation. Similar experiments
479 achieved under increased phosphate levels would be needed to demonstrate a change in calcification
480 and ^{18}O fractionation for this taxon.

481 Carbonate chemistry of the medium is known to influence ^{18}O fractionation (see *4.3.3.* below),
482 potentially accounting for the discrepancy observed. The fact that we harvested cultures at very low
483 cell density ensured that carbonate chemistry remained stable during the experiment and that DIC
484 levels were never limiting (Langer et al. 2006; Barry et al. 2010), results thus being comparable to
485 open ocean settings and transferable to coccoliths in sediments. Once again, no information was
486 provided by Dudley et al. (1986) on cell density or carbonate chemistry parameters so that we are
487 unable to hypothesise on the causes of such different results relying on the nature on the carbonate

system of the medium.

In previous culture studies, growth rate has been shown to have a significant impact on carbon isotope fractionation in coccolith calcite (Ziveri et al., 2003), but effects are less clear for the oxygen isotopes. Ziveri et al. (2003) demonstrated that the effect of growth rate on $\delta^{18}O$ fractionation was high (6 ‰) between the studied species, but smaller within each species. They reached an ambiguous conclusion for *Calcidiscus*: "*Likewise, for C. leptoporus, decreasing irradiance reduced growth rates from 0.7 to 0.2 cells day^{-1}, yet epsilon ^{18}O varied by only 1.5 ‰*". We interpret this isotopic offset as significant as it would lead to a potential 6 °C bias in the temperature estimate. Growth rate differences recorded in the present study both within the same strain grown at different temperatures and between strains at given temperatures were relatively large (0.1 - 0.45 day^{-1}; electronic annex Table A.2), and it is clear that these variations in growth rate were not associated with significantly different ^{18}O fractionation factors.

4.2. Comparison of Temperature Dependence of ^{18}O Fractionation in Cultures and Sediments

Using three clonal laboratory culture strains of *Calcidiscus*, we quantified the effect of temperature on oxygen isotope fractionation in coccoliths of this genus. These culture-based results can be regarded as reliable because relevant parameters were well constrained and isotopes were measured from mono-specific culture residues. We found that ^{18}O fractionation factors were consistent between culture and field studies (Fig. 6). The slopes of the linear regressions represent the sensitivity of ^{18}O fractionation to temperature, which are very similar in both cases: –0.17 ‰ / °C in culture and –0.16 ‰ /°C in sediments (Eq. 3 and Eq. 5). Although these slopes are nearly identical, the near-monogeneric fractions of *Calcidiscus* from sediments exhibit slightly higher $\delta^{18}O$ than the culture residues. This slight offset may be explained by uncertainties inherent to the core top calibration (see *4.3.*).

An offset of –1.1 ‰ separates our culture calibration from the equilibrium line of Kim and O'Neil (1997) corrected for a *p*H of 8.2. This vital effect is rather constant within *Calcidiscus* species and does not vary with the temperature of calcification. This confirms that temperature is the main parameter that controls the intensity of ^{18}O fractionation in coccoliths of this genus. Consequently,

with access to near-monogeneric assemblages of fossil *Calcidiscus* coccoliths, this calibration can be applied as a palaeoproxy for evaluating the temperature of the mixed layer using the culture-based equation.

4.3. Uncertainties associated with the Core Top Calibration

Over the range of temperatures between 15 and 26 °C, the mean oxygen isotope offset between sediment (Eq. 3) and culture (Eq. 5) curves is about 0.34 ‰ (Fig. 6). Translated into a temperature, this would correspond to a potential error of about 1.3 °C in retrieving temperature from Eq. 5. This conservative estimates comprises all the effects of potential biases that are inherent to the use of natural material. This caveat is also encountered for the calibration of foraminiferal $\delta^{18}O$ and Mg/Ca ratio (Bemis et al., 1998; Lea, 2003) or the undersaturation indexes of alkenones (Prahl and Wakeham, 1987; Prahl et al., 2000). For foraminiferal calcite, standard errors are 0.5 °C for $\delta^{18}O$ and 1 °C for Mg/Ca (Lea, 2003) while the error associated with alkenone geothermometry is typically 1.5 °C (Prahl et al., 2006). The standard error of our core top calibration is thus of similar magnitude to that of alkenones, indicating that our palaeotemperature equation affords relatively accurate reconstruction of surface mixed-layer temperatures.

4.3.1. Variability of the Parameters Used for the Calibration

The $\delta^{18}O$ of *Calcidiscus* calcite from seafloor sediments was compared to that of the overlying seawater to determine the amplitude of calcite-seawater ^{18}O fractionation. Mean annual values of $\delta^{18}O_{sw}$ provide a convenient approximation for the calcification environment of *Calcidiscus*, but this may introduce a bias since phytoplankton production is generally not constant through the year. In fact, the extremes of values of $\delta^{18}O$ of surface seawater at our sites indicate very limited seasonal contrast in this parameter (Fig. 5) and the averaged variability for all sites was only 0.026 ‰ (Table 2). Hence, we conclude that seasonal variation in $\delta^{18}O_{sw}$ did not significantly impact our calculated fractionation

543 factors. The overall variation in temperature was relatively high for certain sites between the coldest
544 and warmest seasons, with a mean amplitude of 4.7 °C for all of the studied sites. This translates to an
545 offset of about 2.4 °C between climatic extremes (summer / winter) and annual SSTs (Table 2),
546 corresponding to a maximum potential error of 0.6 ‰ when translated into oxygen isotope
547 fractionation. The use of mean annual values of $\delta^{18}O$ and temperature as used in our calibration is not
548 likely to induce significant errors (see *4.3.2.* and *4.3.3.*). A more appropriate estimate of the impact of
549 temperature and $\delta^{18}O_{sw}$ variation on our core top calibration would require quantification of *C.*
550 *leptoporus* calcification through the year at, or in the vicinity of our sites.
551
552 *4.3.2. Seasonality of Calcidiscus Production*
553
554 The production of *Calcidiscus* and associated flux of coccoliths to the seafloor vary through the year
555 as demonstrated by various sediment trap studies (Broerse et al., 2000a,b; Ziveri et al., 2000; Beaufort
556 and Heussner, 2001; Renaud and Klaas, 2001; Renaud et al., 2002). The $\delta^{18}O$ in coccoliths
557 predominately reflects the temperature of the main season of growth, which may be slightly different
558 from the mean annual temperature used in our calibration. The studies of Renaud et al. (2002) and
559 Broerse et al. (2000a; 2000b) documented the annual evolution of *Calcidiscus* abundance in the
560 vicinity of our studied locations in the North Atlantic Ocean and western Indian Ocean. We used these
561 data to assess the potential bias associated with the use of mean annual temperatures in our calibration.
562 Renaud et al. (2002) and Broerse et al. (2000a) reported that the production of *Calcidiscus* in the
563 North Atlantic varied significantly through the studied time series in 1989-1990. Enhanced abundance
564 of *Calcidiscus* was recorded during the spring between January and May at about 15.5 °C. For sites
565 NABE-48 and NABE-39, the use of the mean annual SST of 17.5 °C may thus induce a maximal 2 °C
566 overestimation of calcification temperature in our calibration. Similarly, for the Somalia sites, highest
567 coccolithophore production was recorded at about 25.5 °C during the autumn (August-November)
568 (Broerse et al., 2000b), a period during which the SST was 1 °C below the mean annual value (~
569 26.5 °C). It must be noted that these data only correspond to snapshots of *Calcidiscus* production and

570 that strong regional contrasts and inter-annual variability in *Calcidiscus* production cannot be
571 excluded. Taken at face value, these observations indicate that the temperatures used for our
572 calibration are an over-evaluation of about 1-2 °C for Atlantic Ocean sites and 1 °C for Indian Ocean
573 sites would represent a maximum error of about 0.5 ‰ in oxygen isotope values. Thus, we
574 hypothesise that the slight offset observed between our core top and culture data (~ 0.3 ‰ in $\delta^{18}O$)
575 (Fig. 6) may result from a seasonal effect.
576
577 *4.3.3. Sensitivity of ^{18}O Fractionation to the Carbonate System*
578
579 Both concentration of bicarbonate ions and *p*H have been shown to effect ^{18}O partitioning in calcite
580 produced by both foraminifera and coccolithophores (Spero et al., 1997, Bijma et al., 1999; Ziveri et
581 al., 2012; see part *2.4.*). A modelling study of the effect of *p*H on $\delta^{18}O_{carb}$ of foraminifera reported a
582 decrease of 1.1 ‰ per *p*H unit increase (Zeebe, 1999). For our study sites, this indicates that a
583 maximum variability of 0.1 ‰ in oxygen isotope fractionation is associated with present-day
584 variability in *p*H of the surface ocean, which ranges from 8.13 ± 0.06 in the North Atlantic (60°W to
585 0°; 0° to 65°N) to 8.07 ± 0.03 in the Indian Ocean (20°E to 120°E; 0° to 25°N) according to Feely et al.
586 (2009). In our study, therefore, the range of *p*H variation was not sufficient to significantly influence
587 ^{18}O fractionation, the maximum potential bias typically being within analytical error.
588 Results from a recent culture experiment have shown that the slope of the linear relationship between
589 $[CO_3^{2-}]$ and $\delta^{18}O$ of *C. leptoporus* calcite is –0.0048 (Ziveri et al., 2012), which translates to a –1 ‰
590 shift in $\delta^{18}O$ with an increase of 208 µmol.kg^{-1} of CO_3^{2-}. The carbonate ion concentration averaged
591 from GLODAP (Key et al., 2004) between 0 and 50 m in our studied locations varied by a maximum
592 of ~50 µmol.kg^{-1}, translating to a maximum potential variability of 0.24 ‰ in ^{18}O fractionation of
593 *Calcidiscus* coccoliths. However, there was no correlation between modern surface water $[CO_3^{2-}]$ and
594 ^{18}O fractionation in our core top calibration, confirming that the potential effect of carbonate ion
595 concentration in seawater was limited. The effect of $[CO_3^{2-}]$ should be taken into account for
596 investigation of time periods marked by strong modification of seawater carbonate chemistry, such as

oceanic acidification events.

4.4. Potential Applications of Coccolith Geochemistry

4.4.1. Palaeoceanographical insights

There has been considerable effort spanning several decades to constrain the evolution of ocean surface temperatures. Since $\delta^{18}O$ values are also influenced by global ice volume and the regional evaporation/precipitation regime, additional isotopic (Δ^{47}) and trace metal (Mg/Ca, Sr/Ca) proxies have been applied to attempt to decouple ice volume and temperature recorded in $\delta^{18}O_{carb}$. Organic-based proxies such as TEX_{86} or alkenone palaeothermometry have also complemented knowledge of the evolution of SSTs (Sachs et al., 2007; Lea, 2003). Extensive species-specific work has been conducted on foraminifera, while very few studies have attempted to produce specific datasets from coccoliths due to the methodological limitation related to their very small size (usually < 20 μm). Recently developed microseparation methods allow purification of coccolith from other components of bulk material (Minoletti et al., 2001; Stoll and Ziveri, 2002; Stoll et al., 2007; Beltran et al., 2007; Minoletti et al., 2009; Hermoso et al., 2009). Beyond generation of coccolith species-specific $\delta^{18}O$ records, this approach is even more necessary when foraminifera are lacking (Oceanic Anoxic Events, high latitude realms) or when they are too rare to be reliably used to represent the $\delta^{18}O$ of seawater (high sedimentation rates, badly preserved shells).

The coccolithophore *Calcidiscus leptoporus* has been present since the Early Miocene (Nannozone NN2; ~ –22.8 Myr). *Calcidiscus leptoporus* coexisted with other (now extinct) species of the genus such as *Calcidiscus macintyrei* and *Calcidiscus tropicus* in the Middle Miocene-Pliocene interval (NN4; –18 Myr to NN19; –0.44 Myr). During the Neogene, the morphology, size and ultrastructure of all of these species remained almost constant (Young, 1998). In our study, no significant difference in oxygen isotope composition was recorded between *C. leptoporus* and *C. quadriperforatus*, species that diverged about 12 Myr ago (Sáez et al., 2003). This suggests that our $\delta^{18}O$ / Temperature calibration

can be applied to all *Calcidiscus* coccoliths covering the range from the Early Miocene to present.

(7) $T\ [°C] = -5.83 \times (\delta^{18}O_{Calcidiscus}\ [V\text{-}PDB] - \delta^{18}O_{sw}\ [V\text{-}SMOW]) + 4.83$

The determination of absolute SSTs still requires knowledge of past $\delta^{18}O_{sw}$. An innovative approach for decoupling changes in temperature and $\delta^{18}O_{sw}$ of the uppermost water column would consist of combining alkenones ($U^{K'}_{37}$) and $\delta^{18}O$ of coccoliths from the same samples, both proxies deriving from same biological group.

The offset between the $\delta^{18}O_{carb}$ of coccoliths and foraminiferal calcite is not always constant through a time slice. This discrepancy is well illustrated by the work of Anderson and Steinmetz (1981) who compared the Pleistocene glacial - interglacial $\delta^{18}O$ records of planktonic foraminifera and of fine fractions (i.e. highly polyspecific coccolith assemblages). In this interval of contrasted climatic cycles, the offset between foraminiferal and coccolith $\delta^{18}O$ is fluctuating and seems to be more limited during glacial than interglacial intervals. Very little is known about the cause of this phenomenon. In the present study, we illustrate the feasibility of concentrating near-monogeneric assemblages of *Calcidiscus*, and of exploiting their oxygen isotope record to attempt reconstructions of palaeotemperatures of the mixed layer. This approach has the potential to help resolving the origin of the discrepancy between coccolith and foraminifera records, and to assess putative ecological and/or biogeochemical controls.

4.4.2. Biogeochemical Insights

In their synthesis of available data on ^{18}O fractionation in coccoliths, Stoll and Ziveri (2004) represented *C. leptoporus* (sensu lato) as the most isotopically offset coccolithophore among twelve other taxa. They quoted a –2.4 ‰ offset from equilibrium using data from Dudley et al. (1986). Using the equilibrium reference of Kim and O'Neil (1997) recalculated for a *p*H of 8.2 (Eq. 2), this offset would be –2.2 ‰. In the present study, the offset was re-evaluated as –1.1 ‰ compared to the same

651 equilibrium conditions.

652 The interspecific offset in ^{18}O fractionation in coccoliths of *Gephyrocapsa oceanica* and *Calcidiscus*
653 spp. is considerable (ca 3 ‰, Fig. A.1). This corresponds to a variability in temperature estimates
654 attributed to the vital effect of about 12 °C. This bias would even be 1-2 °C greater if comparing
655 *Calcidiscus* to *Emiliania huxleyi*, the isotopically heaviest coccolithophore species (Ziveri et al., 2003).
656 One of the main explanations forwarded to account for biologically induced fractionation is the fast
657 growth rate of biogenic carbonates with respect to inorganic precipitation. The faster a mineral grows,
658 the lighter its isotope composition (Weber and Woodhead, 1972; Erez, 1978; McConnaughey, 1989;
659 Adkins et al., 2003; Ziveri et al., 2003). The $\delta^{18}O$ in calcite of most coccolithophore species for which
660 data is available is significantly offset from equilibrium, but the temperature / $\delta^{18}O$ regressions are
661 parallel to equilibrium curves. This more or less constant relationship with the inorganic reference is a
662 consequence of a thermodynamic isotopic process that occurs during partitioning of isotopes
663 integrated into a solid phase (calcification) at the site of coccolith formation. Differences between
664 species can hence be attributed to distinct disequilibria of dissolved carbon species and *p*H in the
665 mineralising fluid compared to the external environment.

666 Based on a charge balance hypothesis, Rickaby et al. (2010) suggested that *Gephyrocapsa oceanica*
667 utilises HCO_3^- as the substrate for calcification, while *Coccolithus pelagicus* may utilise CO_3^{2-}. This
668 hypothesis is supported by the direction of ^{18}O fractionation for these two taxa. There is an offset of
669 about 6.8 ‰ between the equilibrium fractionation of HCO_3^- and CO_3^{2-} with respect to water (Beck et
670 al., 2005), with HCO_3^- being isotopically heavier. This oxygen isotope partitioning between HCO_3^-
671 and CO_3^{2-} is greater than that observed between the $\delta^{18}O$ of coccoliths of the two species (about 1.3 ‰
672 at 17 °C; Ziveri et al., 2003; Rickaby et al., 2010). The vital effect in coccolithophores may thus be the
673 consequence of two processes.

674 Firstly, *G. oceanica* may predominantly use HCO_3^-, but also CO_3^{2-} to a lesser extent (and vice-versa
675 for *C. pelagicus*). The data for *Calcidiscus* would indicate utilisation of CO_3^{2-} for calcification. It is
676 important to note that ^{18}O fractionation for this taxon does not seem to be controlled by the volume of
677 the cell, nor by growth rate. Secondly, the disequilibrium fractionation that occurs upstream of

678 calcification is not the same between species. This phenomenon is prominently caused by kinetic
679 fractionation during trans-membrane CO_2 / HCO_3^- uptake, and may be modulated by the efficiency of
680 Carbon Concentrating Mechanisms (CCMs), a strategy used by phytoplanktonic algae to increase CO_2
681 concentration in the cell with respect to the ambient level evolved to facilitate carbon fixation (Burns
682 and Beardall, 1987; Nimer and Merrett, 1996; Yoshioka, 1997; Giordano et al., 2005). Further work is
683 required to characterise the pools of DIC species involved in coccolithophore calcification, and
684 especially for *Calcidiscus* for which ^{14}C labelling to determine the actual proportion of HCO_3^- and
685 CO_3^{2-} used for calcification, and *p*H measurements of the coccolith vesicle are lacking.
686 A better mechanistic understanding of the disequilibria in coccolithophores for both carbon and
687 oxygen isotopes may prove useful for constraining the carbonate chemistry of surface oceans in the
688 past. Distinct modes of acquisition of DIC lead to species-specific fractionation factors (Ziveri et al.,
689 2003; Stoll and Ziveri, 2004). A change in carbonate chemistry parameters in seawater (*p*H, $[CO_3^{2-}]$)
690 may affect these fractionation coefficients in some species, whereas in others, the fractionation seems
691 to only be influenced by temperature (Rickaby et al., 2010; Ziveri et al., 2012). Interspecific
692 application of the approach used in the present study has clear potential for further constraining the
693 physico-chemical composition of past seawater using the geological record of coccolithophores.
694
695 ## 5. CONCLUSIONS
696
697 Species-specific coccolith isotopic records challenge traditional bulk measurements of carbonate. This
698 justifies the effort to measure coccolithophorid species-specific $\delta^{18}O$ signals. Coccolithophore shells
699 bear geochemical informations that have the potential to help and unravel the isotopic composition
700 and the temperature of the mixed layer, and may represent valuable addition to the foraminiferal
701 record.
702 We successfully achieved the first combined culture and core top calibration of oxygen isotope
703 fractionation in coccolith calcite of the coccolithophore *Calcidiscus* spp. The intensity of this ^{18}O
704 fractionation is strongly and linearly correlated to the temperature of calcification. The good
705 agreement between culture and field studies suggests a robust palaeothermometer of the surface

seawater. Analysing near-monogeneric fractions of *C. leptoporus* concentrated from bulk sediments through the Neogene to Recent interval may provide insightful complementary informations on the temperature and $\delta^{18}O_{sw}$ by applying our culture and field calibration.

The negative isotopic offset from calcite formed at equilibrium conditions of Kim and O'Neil (1997) represents a characteristic of the so-called "light group". This biologically induced fractionation is re-evaluated to –1.1 ‰ for *C. leptoporus* in this study. This offset from equilibrium is likely the consequence of modification of the carbonate chemistry system between seawater and the fluid of the coccolith vesicle upstream to the calcification process. The amplitude of this offset would indicate utilisation of CO_3^{2-} ions as a substrate for calcification in *C. leptoporus*. The temperature and $\delta^{18}O$ regression for *C. leptoporus* and for inorganic calcite have similar slopes, suggesting a final kinetic control of ^{18}O fractionation during the calcification of the coccolith. Further research is required to gain a mechanistic understanding of the assimilation and partitioning of distinct DIC species into the cell.

Acknowledgments. We owe thanks to Grégoire Egoroff for help in microseparating sediments from the Indian Ocean, to Nathalie Labourdette and Norman Charnley for assistance in the laboratory. Guidance from Eva Moreno and Franck Bassinot for the selection of samples and access to the sediment repositories of the MNHN and the LSCE in Paris were appreciated and are sincerely acknowledged. We are grateful to Rusty Lotti (LDEO) for providing us with some of the North Atlantic sediments. Identification of calcareous nannofossils has been facilitated thanks to the Nannotax website (http://nannotax.org/). This study benefited from insightful discussions with Ros Rickaby, Gabrielle Rousselle and Yann Bozec. We thank Jorijntje Henderiks and two anonymous reviewers for constructive and helpful comments, and James McManus for the editorial handling. Coccolithophore strains cultured at Oxford were provided by the Roscoff Culture Collection via funding by the EU FP7 Research Infrastructure Initiative "ASSEMBLE" Ref. 227799. YC was funded by a UPMC "Emergence" Ph.D. studentship and MH is grateful to the Natural Environment Research Council (NERC) for funding through Postdoctoral Fellowship (NE/H015523/1).

734 # 6 – REFERENCES

735 Adkins J. F., Boyle E. A., Curry W. B., and Lutringer A. (2003) Stable isotopes in deep-sea corals and
736 a new mechanism for "vital effects". *Geochim. Cosmochim. Acta* 67, 1129-1143.

737 Anderson T. F. and Steinmetz J. C. (1981) Isotopic and biostratigraphic records of calcareous
738 nannofossils in a Pleistocene core. *Nature* 294, 741-744.

739 Antonov J. I., Seidov D., Boyer T. P., Locarnini R. A., Mishonov A. V., Garcia H. E., Baranova O. K.,
740 Zweng M. M., and Johnson D. R. (2010) *World Ocean Atlas 2009, Volume 2: Salinity* (ed. S.
741 Levitus). NOAA Atlas NESDIS 69, U.S. Government Printing Office, Washington, D.C.

742 Arbuszewski J., de Menocal P., Kaplan A., and Farmer E. C. (2010) On the fidelity of shell-derived
743 delta O-18 (seawater) estimates. *Earth Planet. Sci. Lett.* 300, 185-196.

744 Archer D. E. (1996) An atlas of the distribution of calcium carbonate in sediments of the deep sea.
745 *Global Biogeochem. Cy.* 10, 159-174.

746 Barker S., Cacho L., Benway H., and Tachikawa K. (2005) Planktonic foraminiferal Mg/Ca as a proxy
747 for past oceanic temperatures: a methodological overview and data compilation for the Last
748 Glacial Maximum. *Quat. Sci. Rev* 24, 821-834.

749 Barry J. P., Hall-Spencer J. M., and Tyrell T. (2010) *In situ* perturbation experiments: natural venting
750 sites, spatial/temporal gradients in ocean pH, manipulative in situ pCO_2 perturbations. In
751 *Guide to best practices for ocean acidification research and data reporting* (eds. U. Riebesell,
752 V. J. Fabry, L. Hansson, and J.-P. Gattuso). Publications Office of the European Union,
753 Luxembourg. pp. 123-136.

754 Beaufort L. and Heussner S. (2001) Seasonal dynamics of calcareous nannoplankton on a West
755 European continental margin: the Bay of Biscay. *Mar. Micropaleontol.* 43, 27-55.

756 Beck W. C., Grossman E. L., and Morse J. W. (2005) Experimental studies of oxygen isotope
757 fractionation in the carbonic acid system at 15 degrees, 25 degrees, and 40 degrees C.
758 *Geochim. Cosmochim. Acta* 69, 3493-3503.

759 Beltran C., de Rafélis M., Minoletti F., Renard M., Sicre M. A., and Ezat U. (2007) Coccolith delta O-
760 18 and alkenone records in middle Pliocene orbitally controlled deposits: High-frequency
761 temperature and salinity variations of sea surface water. *Geoch. Geoph. Geosyst.* 8,

762 doi:10.1029/2006GC001483.
763 Beltran C., de Rafélis M., Person A., Stalport F., and Renard M. (2009) Multiproxy approach for
764 determination of nature and origin of carbonate micro-particles so-called “micarb” in pelagic
765 sediments. *Sed. Geol.* 213, 64-76.
766 Bemis B. E., Spero H. J., Bijma J., and Lea D. W. (1998) Reevaluation of the oxygen isotopic
767 composition of planktonic foraminifera: Experimental results and revised paleotemperature
768 equations. *Paleoceanogr.* 13, 150-160, doi:10.1029/98PA00070.
769 Bijma J., Spero H. J., and Lea D. W. (1999) Reassessing foraminiferal stable isotope geochemistry:
770 Impact of the oceanic carbonate system (experimental results). In *Use of Proxies in*
771 *Paleoceanography - Examples from the South Atlantic* (eds. G. Fischer and G. Wefer).
772 Springer, Berlin. pp. 489-512.
773 Bouvier-Soumagnac Y. and Duplessy J. -C. (1985) Carbon and oxygen isotopic composition of
774 planktonic foraminifera from laboratory culture, plankton tows and recent sediment:
775 implications for the reconstruction of paleoclimatic conditions and of the global carbon cycle.
776 *J. Foramin. Res.* 15, 302-320.
777 Broecker W. and Clark E. (2009) Ratio of coccolith CaCO3 to foraminifera CaCO3 in late Holocene
778 deep sea sediments. *Paleoceanogr.* 24, doi:10.1029/2009PA001731.
779 Broecker W. S., Klas M., Clark E., Bonani G., Ivy S., and Wolfli W. (1991) The influence of CaCO3
780 Dissolution on Core Top Radiocarbon Ages for Deep-Sea Sediments. *Paleoceanogr.* 6, 593–
781 608, doi:10.1029/91PA01768.
782 Broerse A. T. C., Brummer G.-J. A., and van Hinte J. E. (2000) Coccolithophore export production in
783 response to monsoonal upwelling off Somalia (northwestern Indian Ocean). *Deep-Sea Res.* 47,
784 2179-2205.
785 Broerse A. T. C., Ziveri P., van Hinte J. E., and Honjo S. (2000) Coccolithophore export production,
786 species composition, and coccolith-CaCO3 fluxes in the NE Atlantic (34°N 21°W and 48°N
787 21°W). *Deep-Sea Res.* 47, 1877-1905.
788 Buitenhuis E. T., Pangerc T., Franklin D. J., Le Quere C., and Malin G. (2008) Growth rates of six
789 coccolithophorid strains as a function of temperature. *Limnol. Oceanogr.* 53, 1181-1185.

790 Burns B. D. and Beardall J. (1987) Utilization of inorganic carbon by marine micro-algae. *J. Exp. Mar.*
791 *Biol. Ecol.* 107, 75-86.
792 Caron D. A., Anderson O. R., Lindsey J. L., Faber W. W., and Lim E. L. (1990) Effects of
793 gametogenesis on test structure and dissolution of some spinose planktonic foraminifera and
794 implications for test preservation. *Mar. Micropaleontol.* 16, 93-116.
795 CLIMAP Project Members (1976) The Surface of the Ice-Age Earth. *Science* 191, 1131-1137.
796 Coplen T. B. (2007) Calibration of the calcite-water oxygen-isotope geothermometer at Devils Hole,
797 Nevada, a natural laboratory. *Geochim. Cosmochim. Acta* 71, 3948-3957.
798 Craig H. (1965) The measurement of oxygen isotope paleotemperatures. In *Stable isotopes in*
799 *oceanographic studies and paleotemperatures* (ed. E. Tongiorgi). Pisa. pp. 3-24.
800 Day C. C. and Henderson G. M. (2011) Oxygen isotopes in calcite grown under cave-analogue
801 conditions. *Geochim. Cosmochim. Acta* 75, 3956-3972.
802 Dera G., Brigaud B., Monna F., Laffont R., Puceat E., Deconinck J.-F., Pellenard P., Joachimski M.
803 M., and Durlet C. (2011) Climatic ups and downs in a disturbed Jurassic world. *Geology* 39,
804 215-218.
805 Dietzel M., Tang J., Leis A., and Koehler S. J. (2009) Oxygen isotopic fractionation during inorganic
806 calcite precipitation - Effects of temperature, precipitation rate and pH. *Chem. Geol.* 268, 107-
807 115.
808 Dudley W. C., Blackwelder P., Brand L., and Duplessy J.-C. (1986) Stable isotopic composition of
809 coccoliths. *Mar. Micropaleontol.* 10, 1-8.
810 Dudley W. C. and Goodney D. E. (1979) Oxygen isotope content of coccoliths grown in culture.
811 *Deep-Sea Res.* 26A, 495-503.
812 Duplessy J. -C., Blanc P. L., and Bé A. W. (1981) Oxygen-18 enrichment of planktonic foraminifera
813 due to gametogenic calcification below the euphotic zone. *Science* 213, 1247-1250.
814 Elderfield H. and Ganssen G. (2000) Past temperature and delta O-18 of surface ocean waters inferred
815 from foraminiferal Mg/Ca ratios. *Nature* 405, 442-445.
816 Emiliani C. (1955) Pleistocene temperatures. *J. Geol.* 63, 538-578.
817 Emiliani C. (1966) Isotopic paleotemperatures. *Science* 154, 851-857.

818 Epstein S., Buchsbaum R., Lowenstam H. A., and Urey H. C. (1951) Carbonate-water isotopic
819 temperature scale. *Geol. Soc. Am. Bull.* 62, 417-426.
820 Epstein S., Buchsbaum R., Lowenstam H. A., and Urey H. C. (1953) Revised carbonate-water isotopic
821 temperature scale. *Geol. Soc. Am. Bull.* 64, 1315-1325.
822 Erez J. (1978) Vital effect on stable-isotope composition seen in foraminifera and coral skeletons.
823 *Nature* 273, 199-202.
824 Erez J. and Luz B. (1983) Experimental paleotemperature equation for planktonic foraminifera.
825 *Geochim. Cosmochim. Acta* 47, 1025-1031.
826 Farmer E. C., Kaplan A., de Menocal P. B., and Lynch-Stieglitz J. (2007) Corroborating ecological
827 depth preferences of planktonic foraminifera in the tropical Atlantic with the stable oxygen
828 isotope ratios of core top specimens. *Paleoceanogr.* 22, doi:10.1029/2006PA001361.
829 Feely R. A., Doney S. C., and Coolet S. R. (2009) Ocean Acidification: Present Conditions and future
830 Changes in a High-CO_2 World. *Oceanography* 22, 36-47.
831 Fischer J., Schott F., and Stramma L. (1996) Currents and transports of the Great Whirl-Socotra Gyre
832 system during the summer monsoon, August 1993. *J. Geophys. Res.* 101, 3573-3587,
833 doi:10.1029/95JC03617
834 Geisen M., Young J. R., Probert I., Saez A. G., Baumann K. H., Sprengel C., Bollmann J., Cros L., De
835 Vargas C., and Medlin L. K. (2004) Species level variation in coccolithophores. In
836 *Coccolithophores: From Molecular Processes to Global Impact* (eds. H. R. Thierstein and J.
837 R. Young). Springer, Berlin. pp. 327-366.
838 Giordano M., Beardall J., and Raven J. A. (2005) CO_2 concentrating mechanisms in algae:
839 Mechanisms, environmental modulation, and evolution. *Annu. Rev. Plant Biol.* 56, 99-131.
840 Gruetzner J., Giosan L., Franz S.-O., Tiedemann R., Cortijo E., Chaisson W. P., Flood R. D., Hagen S.,
841 Keigwin L. D., Poli M.-S., Rio D., and Williams T. (2002) Astronomical age models for
842 Pleistocene drift sediments from the western North Atlantic (ODP Sites 1055-1063). *Mar.*
843 *Geol.* 189, 5-23.
844 Guillard R. R. L. (1975) Culture of phytoplankton for feeding marine invertebrates. In *Culture of*
845 *Marine Invertebrate Animals* (eds. W. L. Smith and M. H. Chanley). Plenum Press, New York.

846 pp. 26-60.
847 Haidar A. T. and Thierstein H. R. (2001) Coccolithophore dynamics off Bermuda (N. Atlantic). *Deep-*
848 *Sea Res.* 48, 1925-1956.
849 Haidar A. T., Thierstein H. R., and Deuser W. G. (2000) Calcareous phytoplankton standing stocks,
850 fluxes and accumulation in Holocene sediments of Bermuda (N. Atlantic). *Deep-Sea Res.* 47,
851 1907-1938.
852 Halloran P. R., Rust N., and Rickaby R. E. M. (2009) Isolating coccoliths from sediment for
853 geochemical analysis. *Geoch. Geoph. Geosyst.* 10, Q03001, doi:10.1029/2008GC002228.
854 Henderson G. M. (2002) New oceanic proxies for paleoclimate. *Earth Planet. Sci. Lett.* 203, 1-13.
855 Hermoso M., Le Callonnec L., Minoletti F., Renard M., and Hesselbo S. P. (2009) Expression of the
856 Early Toarcian negative carbon-isotope excursion in separated carbonate microfractions
857 (Jurassic, Paris Basin). *Earth Planet. Sci. Lett.* 277, 194-203.
858 Hut G. (1987) *Stable Isotope Reference Samples for Geochemical and Hydrological Investigations*.
859 International Atomic Energy Agency, Vienna.
860 Imbrie J., Hays J. D., Martinson D. G., McIntyre A., Mix A. C., Morley J. J., Pisias N. G., Prell W. L.,
861 and Shackleton N. J. (1984) The orbital theory of Pleistocene climate: support from a revised
862 chronology of the marine δ18O record. In *Milankovitch and Climate. Part I* (eds. A. Berger, J.
863 Imbrie, H. Hays, G. Kukla, and B. Saltzman). D. Reidel Publishing, Dordrecht. pp. 269-305.
864 Imbrie J. D., McIntyre A., and Mix A. C. (1989) Oceanic response to orbital forcing in the late
865 Quaternary: observational and experimental strategies. In *Climate and Geosciences, A*
866 *Challenge for Science and Society in the 21th Century* (eds. A. Berger, S. H. Schneider, and
867 J.-C. Duplessy). Kluwer Academic, Boston. pp. 121-164.
868 Kayano K. and Shiraiwa Y. (2009) Physiological regulation of coccolith polysaccharide production by
869 phosphate availability in the coccolithophorid *Emiliania huxleyi*. *Plant Cell Physiol.* 50(8),
870 1522–1531.
871 Keller M. D., Selvin R. C., Claus W., and Guillard R. R. L. (1987) Media for the culture of oceanic
872 ultraphytoplankton. *J. Phycol.* 23, 633-638.
873 Key R. M., Kozyr A., Sabine C. L., Lee K., Wanninkhof R., Bullister J., Feely R. A., Millero F.,

874 Mordy C., and Peng T.-H. (2004) A global ocean carbon climatology: Results from GLODAP.
875 *Global Biogeochem. Cy.* 18, GB4031, doi:10.1029/2004GB002247.
876 Kim S.-T. and O'Neil J. R. (1997) Equilibrium and nonequilibrium oxygen isotope effects in synthetic
877 carbonates. *Geochim. Cosmochim. Acta* 61, 3461-3475.
878 Kloecker R., Ganssen G., Jung S. J. A., Kroon D., and Henrich R. (2006) Late Quaternary millennial-
879 scale variability in pelagic aragonite preservation off Somalia. *Mar. Micropaleontol.* 59, 171-
880 183.
881 Knappertsbusch M. and Brummer G.-J. A. (1995) A sediment trap investigation of sinking
882 coccolithophorids in the North Atlantic. *Deep-Sea Res.* 42, 1083-1109.
883 Knappertsbusch M., Cortes M. Y., and Thierstein H. R. (1997) Morphologic variability of the
884 coccolithophorid *Calcidiscus leptoporus* in the plankton, surface sediments and from the Early
885 Pleistocene. *Mar. Micropaleontol.* 30, 293-317.
886 Koch C. and Young J. (2007) A simple weighing and dilution technique for determining absolute
887 abundances of coccoliths from sediment samples. *J. Nannoplankt. Res.* 29, 67-69.
888 Kucera M. (2007) Chapter Six Planktonic Foraminifera as Tracers of Past Oceanic Environments. In
889 *Developments in Marine Geology* (eds. C. Hillaire-Marcel and A. de Vernal). Elsevier, pp.
890 213-262.
891 Langer G., Geisen M., Baumann K.-H., Klas J., Riebesell U., Thoms S., and Young J. R. (2006)
892 Species-specific responses of calcifying algae to changing seawater carbonate chemistry.
893 *Geoch. Geoph. Geosyst.* 7, doi:10.1029/2005GC001227.
894 Langer G., Oetjen K., and Brenneis T. (2012) Calcification of *Calcidiscus leptoporus* under nitrogen
895 and phosphorus limitation. *J. Exp. Mar. Biol. Ecol.* 413, 131-137.
896 Lea D. W. (2003) Elemental and Isotopic Proxies of Past Ocean Temperatures. In *The Oceans and*
897 *Marine Geochemistry* (ed. H. Elderfield). Elsevier, Amsterdam. pp. 365-390.
898 LeGrande A. N. and Schmidt G. A. (2006) Global gridded data set of the oxygen isotopic composition
899 in seawater. *Geophys. Res. Lett.* 33, L12604, doi:10.1029/2006GL026011.
900 Locarnini R. A., Mishonov A. V., Antonov J. I., Boyer T. P., Garcia H. E., Baranova O. K., Zweng M.
901 M., and Johnson D. R. (2010) *World Ocean Atlas 2009, Volume 1: Temperature* (ed. S.

902 Levitus). NOAA Atlas NESDIS 68, U.S. Government Printing Office, Washington, D.C.
903 Mathien-Blard E. and Bassinot F. (2009) Salinity bias on the foraminifera Mg/Ca thermometry:
904 Correction procedure and implications for past ocean hydrographic reconstructions. *Geoch.*
905 *Geoph. Geosyst.* 10, Q12011, doi:10.1029/2008GC002353.
906 McConnaughey T. (1989) 13C and 18O isotopic disequilibrium in biological carbonates: I. Patterns.
907 *Geochim. Cosmochim. Acta* 53, 151-162.
908 McIntyre A. and McIntyre R. (1970) Coccolith concentration and differential solution in oceanic
909 sediments. In *Micropaleontology of the Oceans* (eds. B. M. Funnel and W. R. Riedel).
910 Cambridge University Press, Cambridge. pp. 253-261.
911 Mekik F., Noll N., and Russo M. (2010) Progress toward a multi-basin calibration for quantifying
912 deep sea calcite preservation in the tropical/subtropical world ocean. *Earth Planet. Sci. Lett.*
913 299, 104-117.
914 Minoletti F., Gardin S., Nicot E., Renard M., and Spezzaferri S. (2001) A new experimental protocol
915 for granulometric separation of calcareous nannofossils assemblages: paleoecological and
916 geochemical applications. *Bull. Soc. géol. Fr.* 172, 437-446.
917 Minoletti F., de Rafélis M., Renard M., and Gardin S. (2004) Remaniement des nannofossiles
918 calcaires maastrichtiens dans les sédiments du Danien basal de Bidart (France): arguments
919 isotopiques (carbone et oxygène). *Revue de Micropaléontologie* 47, 145-152.
920 Minoletti F., de Rafelis M., Renard M., Gardin S., and Young J. (2005) Changes in the pelagic fine
921 fraction carbonate sedimentation during the Cretaceous-Paleocene transition: contribution of
922 the separation technique to the study of Bidart section. *Palaeogeogr. Palaeoclimatol.*
923 *Palaeoecol.* 216, 119-137.
924 Minoletti F., Hermoso M., and Gressier V. (2009) Separation of sedimentary micron-sized particles
925 for palaeoceanography and calcareous nannoplankton biogeochemistry. *Nat. Protoc.* 4, 14-24.
926 Nancollas G. H. and Reddy M. M. (1971) The crystallization of calcium carbonate II. Calcite growth
927 mechanism. *J. Colloid Interface Sci.* 36, 166-172.
928 Nimer N. A. and Merrett M. J. (1996) The development of a CO_2-Concentrating Mechanism in
929 Emiliania huxleyi. *New Phytol.* 133, 383-389.

930 O'Neil J. R., Clayton R. N., and Mayeda T. K. (1969) Oxygen isotope fractionation in divalent metal
931 carbonates. *J. Chem. Phys.* 51, 5547-5558.
932 Peeters F. J. C., Brummer G.-J. A., and Ganssen G. (2002) The effect of upwelling on the distribution
933 and stable isotope composition of *Globigerina bulloides* and *Globigerinoides ruber* (planktic
934 foraminifera) in modern surface waters of the NW Arabian sea. *Global Planet. Change* 34,
935 269-291.
936 Prahl F. G. and Wakeham S. G. (1987) Calibration of unsaturation patterns in long-chain ketone
937 compositions for paleotemperature assessment. *Nature* 330, 367-369.
938 Prahl F. G., Dymond J., and Sparrow M. A. (2000) Annual biomarker record for export production in
939 the central Arabian Sea. *Deep-Sea Res.* 47, 1581-1604.
940 Prahl F. G., Mix A. C., and Sparrow M. A. (2006) Alkenone paleothermometry: Biological lessons
941 from marine sediment records off western South America. *Geochim. Cosmochim. Acta* 70,
942 101-117.
943 Probert I. and Houdan A. (2004) The laboratory culture of coccolithophores. In *Coccolithophores:*
944 *From Molecular Processes to Global Impact* (eds. H. R. Thierstein and J. Young). Springer,
945 Berlin. pp. 217-249.
946 Renaud S. and Klaas C. (2001) Seasonal variations in the morphology of the coccolithophore
947 *Calcidiscus leptoporus* off Bermuda (N. Atlantic). *J. Plankton. Res.* 23, 779-795.
948 Renaud S., Ziveri P., and Broerse A. T. C. (2002) Geographical and seasonal differences in
949 morphology and dynamics of the coccolithophore *Calcidiscus leptoporus*. *Mar.*
950 *Micropaleontol.* 46, 363-385.
951 Rickaby R. E. M., Henderiks J., and Young J. (2010) Perturbing phytoplankton: response and isotopic
952 fractionation with changing carbonate chemistry in two coccolithophore species. *Clim. Past* 6,
953 771-785.
954 Sabine C. L., Key R. M., Kozyr A., Feely R. A., Wanninkhof R., Millero F. J., Peng T.-H., Bullister J.,
955 and Lee K. (2005) *Global Ocean Data Analysis Project: Results and Data*. ORNL/CDIAC-
956 145, NDP-083. Carbon Dioxide Information Analysis Center, Oak Ridge National Laboratory,
957 U.S. Department of Energy, Oak Ridge, Tennessee.

958 Sachs J. P., Pahnke K., Smittenberg R. and Zhang Z. (2007) Biomarker Indicators of Past Climate. In
959 *Encyclopedia of Quaternary Science* (ed. S. Elias). Elsevier, Amsterdam.
960 Saez A. G., Probert I., Geisen M., Quinn P., Young J. R., and Medlin L. K. (2003) Pseudo-cryptic
961 speciation in coccolithophores. *Proc. Natl. Acad. Sci. USA* 100, 7163-7168.
962 Schlitzer R. (2008) Ocean Data View. http://odv.awi.de.
963 Schneidermann N. (1977) Selective dissolution of recent coccoliths in the Atlantic Ocean. In *Oceanic*
964 *Micropaleontology* (ed. A. T. S. Ramsay). Academic Press, London. pp. 1009-1053.
965 Schott F., McCreary J., and Julian P. (2001) The monsoon circulation of the Indian Ocean. *Prog.*
966 *Oceanogr.* 51, 1-123.
967 Spero H. J., Bijma J., Lea D. W., and Bemis B. E. (1997) Effect of seawater carbonate concentration
968 on foraminiferal carbon and oxygen isotopes. *Nature* 390, 497-500.
969 Spero H. J. and Lea D. W. (1993) Intraspecific stable isotope variability in the planktic foraminifera
970 *Globigerinoides sacculifer*. Results from laboratory experiments. *Mar. Micropaleontol.* 22,
971 221-234.
972 Stoll H. M., Ziveri P., Shimizu N., Conte M., and Theroux S. (2007) Relationship between coccolith
973 Sr/Ca ratios and coccolithophore production and export in the Arabian Sea and Sargasso Sea.
974 *Deep-Sea Res.* 54, 581-600.
975 Stoll H. M. and Ziveri P. (2002) Separation of monospecific and restricted coccolith assemblages from
976 sediments using differential settling velocity. *Mar. Micropaleontol.* 46, 209-221.
977 Stoll H. and Ziveri P. (2004) Coccolithophore-based geochemical proxies. In *Coccolithophores: From*
978 *Molecular Processes to Global Impact* (eds. H. R. Thierstein and J. Young). Springer, Berlin.
979 pp. 529-562.
980 Tomczak M. and Godfrey J. S. (1994) *Regional Oceanography: an Introduction*. Pergamon, Oxford.
981 Urey H. C. (1947) The thermodynamic properties of isotopic substances. *J. Chem. Soc*, 562-581.
982 Urey H. C., Lowenstam H. A., Epstein S., and McKinney C. R. (1951) Measurement of
983 paleotemperatures and temperatures of the Upper Cretaceous of England, Denmark, and the
984 southeastern United States. *Geol. Soc. Am. Bull.* 62, 399-416.
985 Vénec-Peyré M.-T., Caulet J. P., and Grazzini C. V. (1995) Paleohydrographic changes in the Somali

Basin (5°N upwelling and equatorial areas) during the last 160 kyr, cased on correspondence analysis of foraminiferal and radiolarian assemblages. *Paleoceanogr.* 10, 473-491, doi:10.1029/95PA00420.

Wang Y., Cheng H., Edwards R. L., Kong X., Shao X., Chen S., Wu J., Jiang X., Wang X., and An Z. (2008) Millennial- and orbital-scale changes in the East Asian monsoon over the past 224,000 years. *Nature* 451, 1090-1093.

Weber J. N. and Woodhead P. M. (1972) Temperature dependance of oxygen 18 concentration in reef coral carbonates. *J. Geophys. Res.* 77, 463-473, doi:10.1029/JC077i003p00463.

Wefer G. and Berger W. H. (1991) Isotope paleontology: growth and composition of extant calcareous species. *Mar. Geol.* 100, 207-248.

Wolf-Gladrow D. A., Bijma J., and Zeebe R. E. (1999) Model simulation of the carbonate chemistry in the microenvironment of symbiont bearing foraminifera. *Mar. Chem.* 64, 181-198.

Yoshioka T. (1997) Phytoplanktonic carbon isotope fractionation: equations accounting for CO_2-concentrating mechanisms. *J. Plankton. Res.* 19, 1455-1476.

Young J. (1998) Neogene. In *Calcareous Nannofossil Biostratigraphy* (ed. P. R. Bown). Chapman & Hall, London. pp. 225-265.

Young J. and Ziveri P. (2000) Calculation of coccolith volume and its use in calibration of carbonate flux estimates. *Deep-Sea Res.* 47, 1679-1700.

Zachos J. C., Dickens G. R. and Zeebe R. E. (2008) An early Cenozoic perspective on greenhouse warming and carbon-cycle dynamics. *Nature* 451, 279-283.

Zachos J. C., Pagani M., Sloan L., Thomas E., and Billups K. (2001) Trends, rhythms, and aberrations in global climate 65 Ma to present. *Science* 292, 686-693.

Zeebe R. E. (1999) An explanation of the effect of seawater carbonate concentration on foraminiferal oxygen isotopes. *Geochim. Cosmochim. Acta* 63, 2001-2007.

Zeebe R. E. and Wolf-Gladrow D. (2001) *CO2 in seawater: equilibrium, kinetics, isotopes*. Elsevier, Amsterdam.

Ziveri P., Broerse A. T. C., van Hinte J. E., Westbroek P., and Honjo S. (2000) The fate of coccoliths

at 48°N 21°W, northeastern Atlantic. *Deep-Sea Res.* 47, 1853-1875.

Ziveri P., Stoll H., Probert I., Klaas C., Geisen M., Ganssen G., and Young J. (2003) Stable isotope vital effects in coccolith calcite. *Earth Planet. Sci. Lett.* 210, 137-149.

Ziveri P., Thoms S., Probert I., Geisen M., and Langer G. (2012) A universal carbonate ion effect on stable oxygen isotope ratios in unicellular planktonic calcifying organisms. *Biogeosciences* 9, 1025-1032.

Figure and Table captions

Figure 1: Map showing the locations of the studied core top sediments. Site locations (black stars) are plotted on regional bathymetric maps of the Atlantic (a) and Indian (b) Oceans. The main surface currents (after Tomczak and Godfrey, 1994) are indicated by bold black arrows: the North Atlantic Current (NAC), the Azores Current (AC), the Portugal Current (PC) and the Canary Current (CC), the South Equatorial Current (SEC), the Zanzibar Current (ZC), the Somalia Current (SC), the East Arabian Current (EAC) and the Southwest Monsoon Current (SMC). The dashed red lines and numbers represent surface water isotherms. The studied sites cover a wide range of temperatures used for generating our core top calibration of *Calcidiscus* ^{18}O fractionation. Maps were generated using Ocean Data View package version 4.3.7. (Schlitzer, 2008).

Figure 2: Oxygen isotope fractionation of *Calcidiscus* strains grown in culture at distinct temperatures. The magnitude of ^{18}O fractionation for each temperature is expressed as the isotopic difference between coccoliths expressed in V-PDB and the medium expressed in V-SMOW (left axis) and reported as the ε notation (right axis). Regression through all of the culture data of the present study and the narrow 95 % confidence interval indicate a strong temperature dependence on the intensity of ^{18}O fractionation ($r = 0.98$; RMSE = 0.8 °C). This relationship is described by the equation $\delta^{18}O_{carb} - \delta^{18}O_{medium} = -0.17 \times T + 0.83$. A panel showing the correspondence between the symbols and the various strains of *Calcidiscus* grown in this and previous studies is inset top right. This fractionation factor or "vital effect" of –1.1 ‰ ("light group") is substantially different than that from

1041 the pioneering study of Dudley et al. (1986). Equilibrium calcite ^{18}O fractionation with temperature (cf.
1042 Eq. 2 in text) is calculated after Kim and O'Neil (1997), and adjusted for a *p*H 8.2. A rather constant
1043 offset is observed between *Calcidiscus* and equilibrium conditions, and is not influenced by the
1044 temperature (see electronic annex Fig. A.1 for a representation of a variety of equilibrium lines given
1045 in the literature).
1046
1047 Figure 3: Depth profiles of seawater temperature (a) and $\delta^{18}O_{sw}$ (b) between 0 and 150 metres.
1048 The Atlantic and Indian Ocean sites are plotted using open and plain symbols, respectively. The
1049 shaded area corresponds to the calcification zone of *Calcidiscus* (0-50 m depth after Knappertsbusch
1050 and Brummer, 1995; Haidar et al., 2000; Haidar and Thierstein, 2001). The characteristics of the 0-50
1051 m water mass were averaged to determine mean annual values of temperature and $\delta^{18}O_{sw}$. These
1052 parameters serve as the seawater reference for calculating ^{18}O fractionation for *Calcidiscus* spp. in our
1053 core top calibration, and for calculating the $\delta^{18}O$ of the equilibrium calcite.
1054
1055 Figure 4: Bulk sediment and fraction obtained by the microseparation technique (Minoletti et al.,
1056 2009) from SU90-03 core top sediment from the Northern Atlantic Ocean. a) Highly
1057 heterogeneous and polyspecific assemblage of the bulk sample observed using polarised microscopy.
1058 This micrograph illustrates the relatively low abundance of the target *Calcidiscus* spp. in the bulk
1059 sample (relative abundance of ~ 5 % determined by optical counts from > 500 particles). b) Scanning
1060 Electron Microscope view of the same bulk assemblage. Non-*Calcidiscus* coccoliths recognised in this
1061 image are from the genera *Pontosphaera*, *Umbilicosphaera*, *Gephyrocapsa* and *Emiliania*. c) Smear-
1062 slide observation of a 3-5 µm microseparated fraction showing the high abundance of *Calcidiscus*
1063 *leptoporus* (~ 80 %). In this example, *Calcidiscus* is enriched ~ 16-fold with respect to the bulk
1064 assemblage. d) Scanning Electron Microscope view of the same microseparated fraction showing a
1065 close-up of *C. leptoporus* specimens (morphotype "Intermediate" sensu Knappertsbusch et al., 1997).
1066 The preservation is relatively good, albeit with some etching, but no recrystallisation is observed on
1067 the coccoliths.

Figure 5: Oxygen isotope fractionation between *Calcidiscus*-dominated fractions and seawater (averaged over 0-50 m depth range). Left: the grey-shaded area corresponds to ^{18}O fractionation between *Calcidiscus* calcite (red filled circles) and seawater $\delta^{18}O$ (blue dashed line). Right: mean annual temperature (vertical solid line) and seasonal extremes (grey shaded area) recorded over the range of calcification depth of *Calcidiscus* spp.

Figure 6: Core top and culture calibration of ^{18}O fractionation in *Calcidiscus* calcite. $\delta^{18}O$ of near-monogeneric assemblages of *Calcidiscus* from core tops (red circles) are strongly correlated to SSTs 0-50 m. This linear relationship is described by the equation $\delta^{18}O_{carb} - \delta^{18}O_{sw} = -0.16 \times T + 0.97$ ($r = 0.94$). The culture (black diamonds) and field approaches give concordant results on ^{18}O fractionation with respect to temperature. The higher variability for the in situ dataset (RMSE = 1.4 °C) compared to culture data (RMSE = 0.8 °C) might be explained by uncertainties in retrieving environmental parameters and a possible effect of seasonality.

Table 1: Location, water column parameters and age control of studied samples. Mean annual SSTs at 0 m are from the World Ocean Atlas 2009 (Locarnini et al., 2010). The saturation state of bottom water with respect to calcium carbonate ($\Delta[CO_3^{2-}]$) was calculated from GLODAP (Key et al., 2004; Sabine et al., 2005) using the Ocean Data View package version 4.3.7. (Schlitzer, 2008). The age of each studied sediment was less than 5 kyr (see associated references).

Table 2: Variability of temperature and $\delta^{18}O_{sw}$ of surface seawater at each location. Averaged temperatures and $\delta^{18}O_{sw}$ are given for the interval 0-50 metres where *Calcidiscus* calcifies. $\Delta\delta^{18}O_{sw}$ is calculated from gridded salinity data (WOA09, Antonov et al., 2010) applying the empirical $\delta^{18}O_{sw}$ / salinity relationship ($\delta^{18}O_{sw} = 0.55 \times$ Salinity $- 18.98$ for the Atlantic sites and $\delta^{18}O_{sw} = 0.16 \times$ Salinity $- 5.31$ for the Indian sites) from LeGrande and Schmidt (2006). Extremes of these parameters (ΔT;

1094 $\Delta\delta^{18}O_{sw}$) retrieved for warmest and coldest periods were used to infer the seasonal variability of the
1095 environmental parameters, which may influence ^{18}O fractionation.
1096
1097 **Table 3: Composition of microseparated fractions.** For each fraction, the relative abundance of
1098 *Calcidiscus* spp. was estimated from smear-slide observation with polarised microscopy. Counts were
1099 made from at least 500 particles to ensure statistical reliability. A mean enrichment factor of 13
1100 (relative abundance of *Calcidiscus* spp. in the fraction compared to that measured in bulk samples, i.e.
1101 ~ 5 %) was obtained in this study. Secondary components coexisting in the fractions are given in the
1102 right column of the table.
1103
1104 ## Appendix – Electronic Annexes
1105
1106 **Figure A.1: Oxygen isotope fractionation of coccoliths and equilibrium calcites between 14 and**
1107 **28°C.** The temperature dependence of ^{18}O fractionation is expressed as the ε notation on the left axis,
1108 and as the α notation on the right axis. The red curves represent two coccolithophorid species with the
1109 equations of the linear regressions. *Gephyrocapsa oceanica* belongs to the heavy group with $\delta^{18}O$
1110 values greater than equilibrium (data from Ziveri et al., 2003). The data of the present study for
1111 *Calcidiscus* spp. confirms that this taxon belongs to the "light group" with a re-evaluated offset of –
1112 1.1‰ from the equilibrium line (7) of Kim and O'Neil (1997) corrected for a seawater at *p*H 8.2. Both
1113 coccolith curves are parallel to each other, and their slopes show identical trends compared to the
1114 equilibrium curves. Equation (7) has been used as "one" equilibrium condition in the present study,
1115 being the most commonly used in palaeoceanographic studies.
1116
1117 **Table A.1**: Physical and chemical properties (Temperature, $\delta^{18}O_{sw}$, $[CO_3^{2-}]$) for each studied locations.
1118
1119 **Table A.2**: Oxygen isotopic composition of the *Calcidiscus* spp. calcite grown at distinct temperatures.
1120 Classification of distinct morphotypes after Knappertsbusch et al. (1997). Oxygen isotopic

composition and *p*H of the culturing medium. The growth rate, commonly termed mu was calculated as: $\mu = (\ln C1 - \ln C0) / T$ where C0 is in initial cell density (number of cells per millilitre of medium) at inoculation, and C1 the cell density at the end. The final *p*H of the medium is expressed using the total scale notation. N/A: Data Non Available.

Table A.3: Stable oxygen and carbon isotopic composition of the bulk and separated fractions from core tops. Fractions 2-5 µm from sample AT960028, and 5-8 µm from NO75-14, VM30-76, SU81-28 were discarded due to their too low relative abundances in *Calcidiscus* coccoliths.

Candelier et al. - Table 1

Site	Campaign	Latitude	Longitude	Water depth (m)	Mean annual SST (°C)	Bottom water ΔCO_3^{2-}(µmol.kg-1)	Age control (kyr)	
SU90-03	PALEOCINAT	40°05N	32°W	2475	18.4	39.5	0 - 4	Mathien-Blard and Bassinot, 2009
SU90-08	PALEOCINAT	43°83N	30°58W	3080	16.4	39.4	0 - 4	Mathien-Blard and Bassinot, 2009
VM04-08	LDEO V04	37°23N	33°13W	1697	19.8	44.6	0 - 5	CLIMAP Project Members, 1976
VM30-76	LDEO V30	33°60N	31°48W	3567	21.2	30.3	0 - 0.5	Broecker et al., 1991
VM30-97	LDEO V30	41°00N	32°93W	3371	18.1	26.8	0 - 1	Imbrie et al., 1989
MD95-2038	IMAGES 1-MD101	37°75N	27°18W	2310	18.6	47.7	0 - 4	Mathien-Blard and Bassinot, 2009
SU81-28	CEPAG	40°59N	10°51W	4020	16.5	35.3	0 - 0.5	Broecker et al., 1991
NO75-14	TRANSAT	34°41N	61°27W	4355	22.5	3.5	0 - 2	Grutzner et al., 2002
MD104-AT960029	PEGASE MD104	10°56N	52°37E	3140	26.3	-0.9	0 - 1.5	Vénec-Peyré et al., 1995
MD104-AT960028	PEGASE MD104	4°21N	49°15E	2576	26.7	-1.2	0 - 0.5	Klöcker et al., 2006

Candelier et al. - Table 2

	Annual mean value (0-50m depth range)		Seasonal variability			
			Warm season		Cold season	
Site	T(°C)	$\delta^{18}O_{sw}$ (‰)	ΔT (°C)	$\Delta\delta^{18}O_{sw}$ (‰)	ΔT (°C)	$\Delta\delta^{18}O_{sw}$ (‰)
SU90-03	17.7	0.83	+2.7	+0.01	-2.1	-0.01
SU90-08	16.2	0.74	+2.4	+0.01	-1.9	-0.01
VM04-08	18.9	0.95	+2.7	+0.02	-2.3	-0.03
VM30-76	20.6	1.08	+2.5	+0.03	-2.2	-0.03
VM30-97	17.6	0.81	+2.7	+0.02	-2.2	-0.01
MD95-2038	18.2	0.93	+2.4	+0.04	-2.3	-0.03
SU81-28	15.9	0.77	+1.9	-0.02	-1.9	+0.02
NO75-14	22.0	1.07	+3.2	-0.04	-2.7	+0.03
MD104-AT960029	25.7	0.54	+2.0	+0.05	-2.7	-0.05
MD104-AT960028	26.5	0.49	+1.7	+0.02	-1.9	-0.03

Candelier et al. - Table 3

Sample	Size fraction	*C. leptoporus* relative abundance (%)	Secondary components in fractions (by order of abundance)
SU90-03-1	3-5µm	80	*Gephyrocapsa* spp., *E. huxleyi*
SU90-03-1	5-8µm	86	*C. pelagicus, Helicosphaera* spp., *Pontosphaera* spp.
SU90-03-2	3-5µm	82	*Gephyrocapsa* spp., *E. huxleyi*
SU90-03-2	5-8µm	71	*C. pelagicus, Helicosphaera spp., Pontosphaera* spp.
SU90-08-1	3-5µm	85	*Gephyrocapsa* spp., *E. huxleyi*
SU90-08-1	5-8µm	82	*Helicosphaera* spp., *C. pelagicus, Pontosphaera* spp.
SU90-08-2	3-5µm	82	*Gephyrocapsa* spp., *E. huxleyi*
SU90-08-2	5-8µm	83	*Healicosphaera* spp., *C. pelagicus, Pontosphaera* spp.
SU90-08-3	3-5µm	68	*Gephyrocapsa* spp., *E. huxleyi*
SU90-08-3	5-8µm	74	*Helicosphaera* spp., *Pontosphaera* spp., *C. pelagicus*
VM04-08	3-5µm	78	*Helicosphaera* spp., *Umbilicosphaera* spp., *Gephyrocapsa* spp.
VM04-08	5-8µm	54	*Gephyrocapsa* spp., *E. huxleyi,* Foraminiferal fragments
VM30-76	3-5µm	68	*Umbilicosphaera* spp., *Gephyrocapsa* spp
VM30-97	3-5µm	71	*Gephyrocapsa* spp., *E.huxleyi, Umbilicosphaera* spp.
VM30-97	5-8µm	56	*C. pelagicus,* Foraminiferal fragments
MD95-2038-1	3-5µm	62	*Gephyrocapsa* spp., *E.huxleyi*
MD95-2038-1	5-8µm	73	*Helicosphaera* spp., *Pontosphaera* spp., *C. pelagicus*
SU81-28	3-5µm	61	*Gephyrocapsa* spp., *Helicosphaera* spp., Foraminiferal fragments
NO75-14	3-5µm	50	*Helicosphaera* spp., *Umbilicosphaera* spp., Foraminiferal fragments
MD104-AT960029-1	3-5µm	60	*Gephyrocapsa* spp., *E. huxleyi,* Foraminiferal fragments
MD104-AT960029-1	5-8µm	80	Foraminiferal fragments, *Helicosphaera* spp.
MD104-AT960029-2	3-5µm	47	*Gephyrocapsa* spp., *E. huxleyi,* Foraminiferal fragments
MD104-AT960029-2	5-8µm	53	Foraminiferal fragments
MD104-AT960028-1	5-8µm	65	Foraminiferal fragments, *Helicosphaera* spp.

Candelier et al. - Figure 1

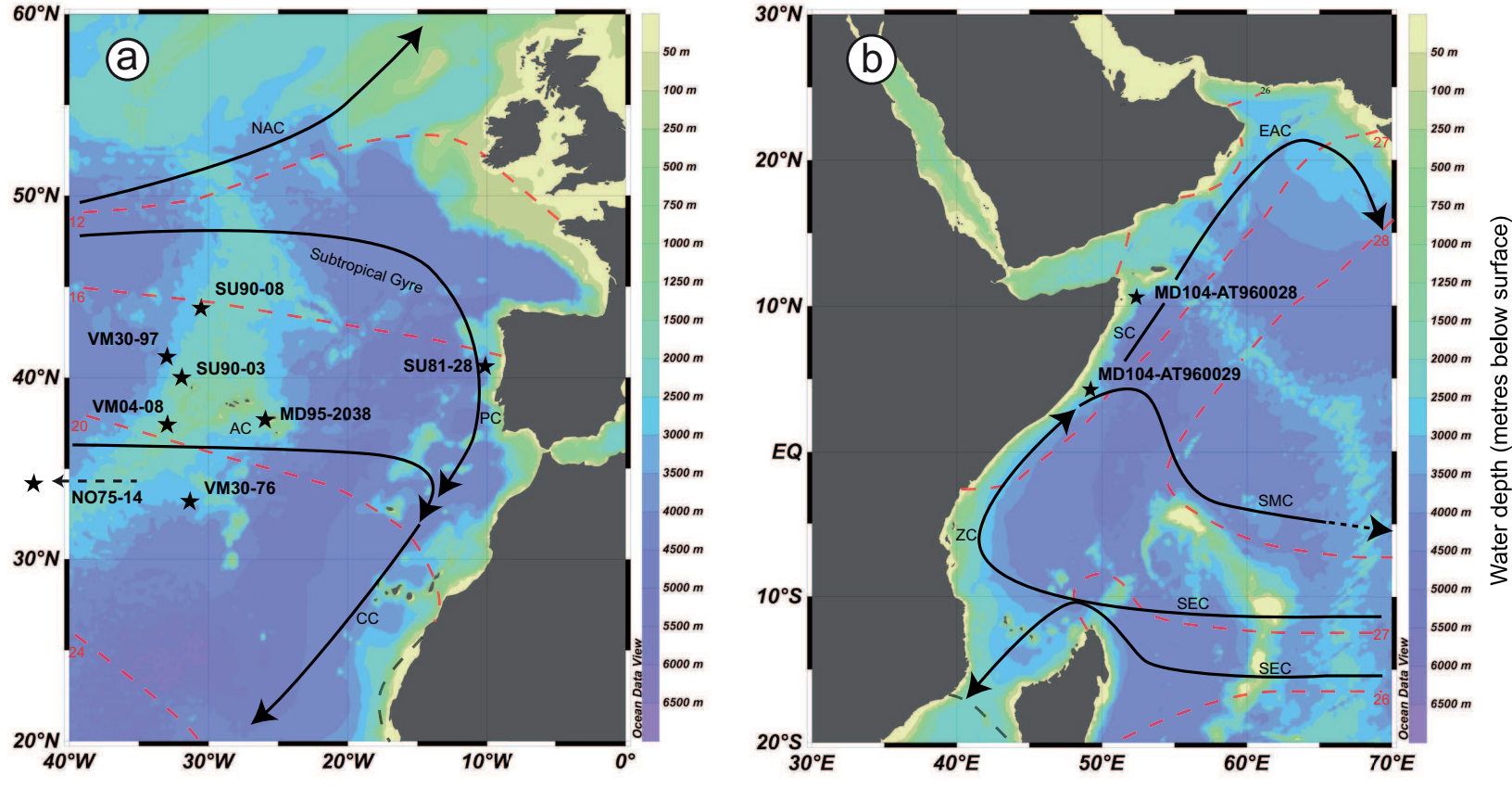

Candelier et al. - Figure 2

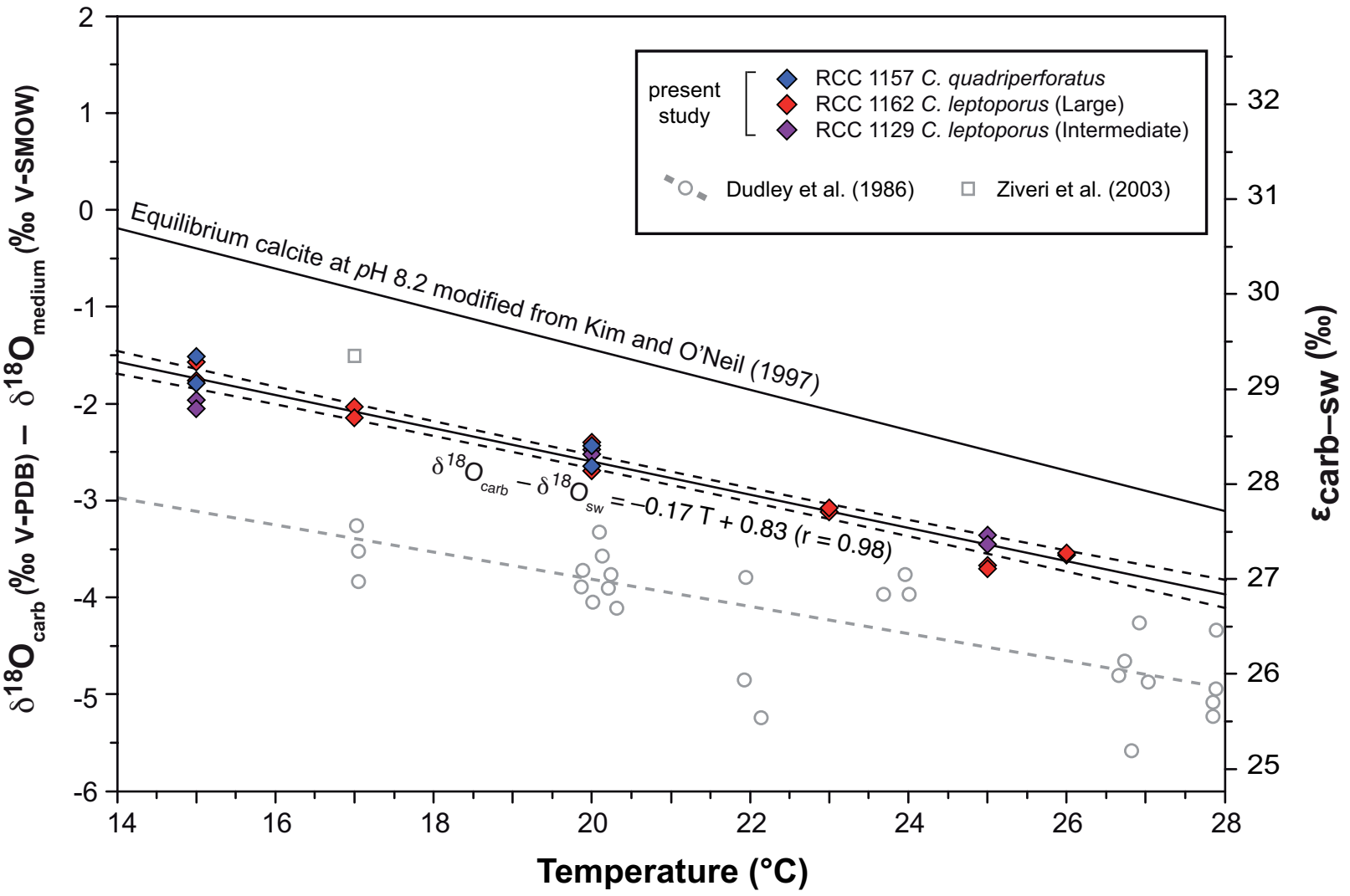

Candelier et al. - Figure 3

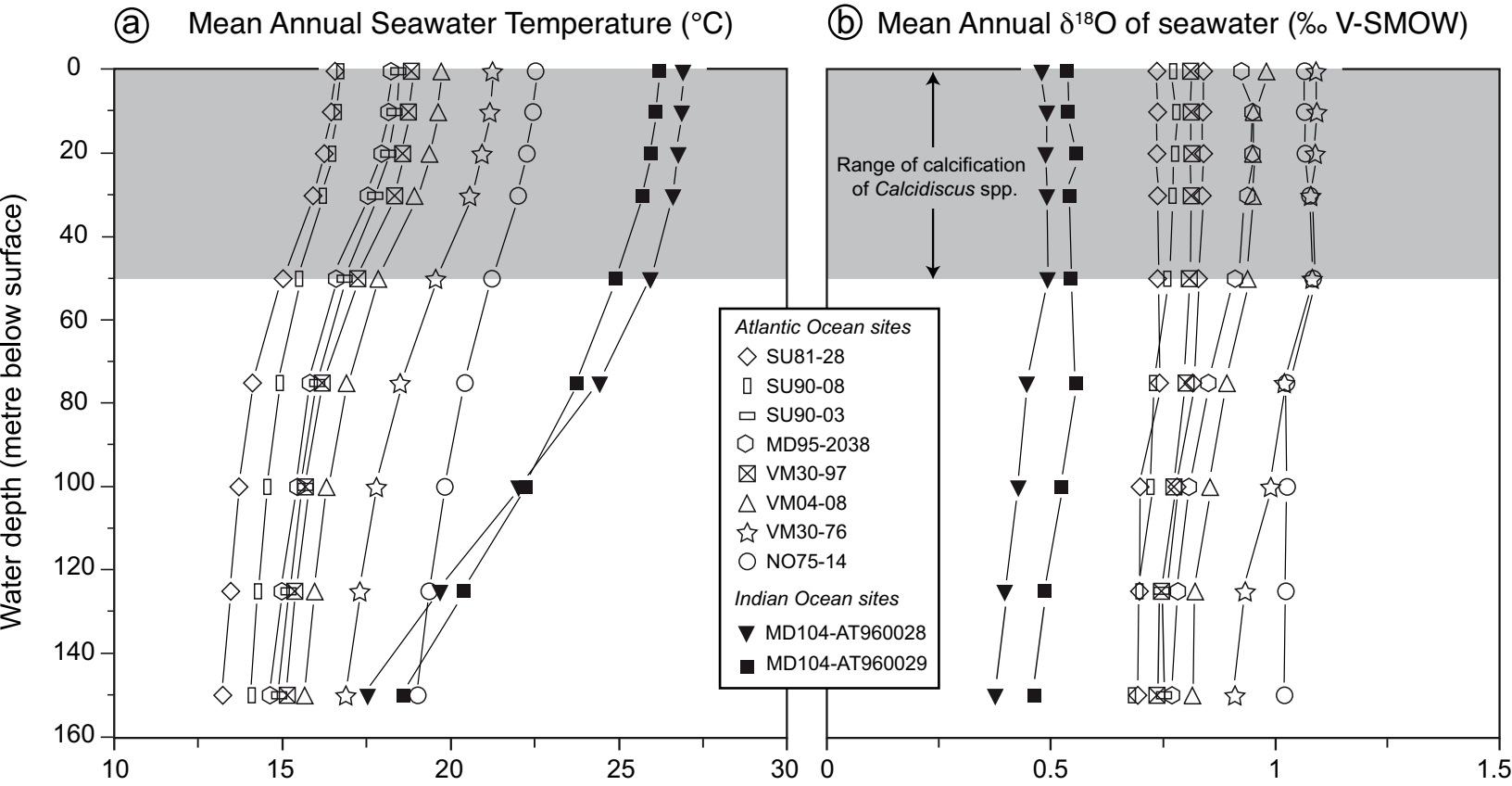

Candelier et al. - Figure 4

Click here to download high resolution image

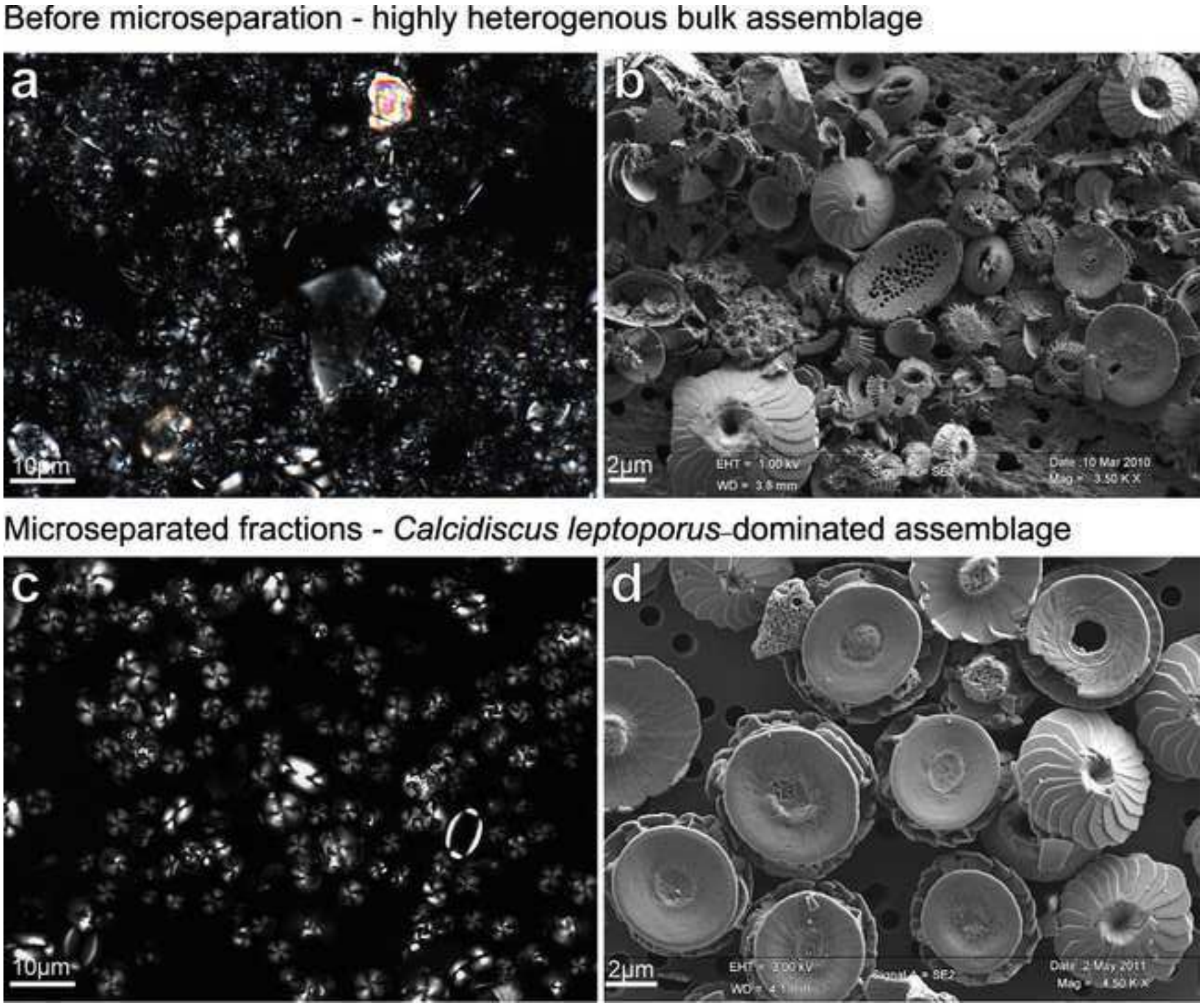

Candelier et al. - Figure 5

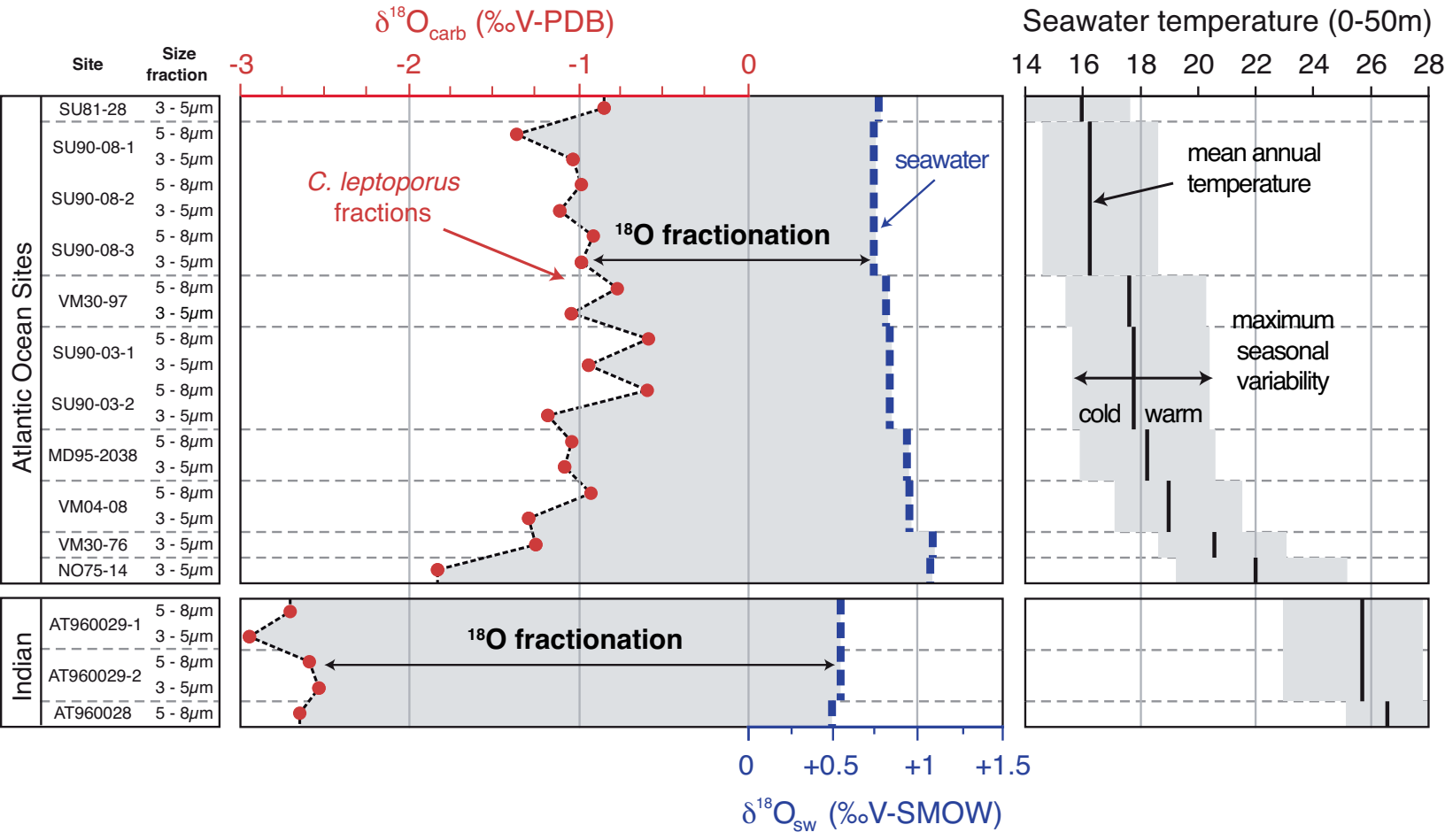

Candelier et al. - Figure 6